Fusion Engineering and Design 23 (1993) 251–297
North-Holland

Critical technical issues and evaluation and comparison studies for inertial fusion energy reactors

M.A. Abdou [a], A.Y. Ying [a], M.S. Tillack [a], N.M. Ghoniem [a], L.M. Waganer [b], D.E. Driemeyer [b], G.J. Linford [c] and D.J. Drake [d]

[a] *Mechanical, Aerospace and Nuclear Engineering Department, University of California, Los Angeles, Los Angeles, California, USA*
[b] *McDonnell Douglas Aerospace, St. Louis, Missouri, USA*
[c] *TRW Space and Electronics Division, Redondo Beach, California, USA*
[d] *Formerly of KMS Fusion Inc., Ann Arbor, Michigan, USA*

Submitted 30 July 1993, revised version 1 September 1993; accepted 2 September 1993

The critical technical issues, evaluation and comparison of two inertial fusion energy (IFE) reactor design concepts developed in the Prometheus studies are presented. The objectives of this study were (1) to identify and characterize the critical issues and the R&D required to resolve them, and (2) to establish a sound basis for future IFE technical and programmatic decisions by evaluating and comparing the different design concepts. Each critical issue contains several key physics and engineering issues associated with the major reactor components and impacts key aspects of feasibility, safety, and economic potential of IFE reactors. Generic critical issues center around: (1) demonstration of moderate gain at low driver energy, (2) feasibility of direct drive targets, (3) feasibility of indirect drive targets for heavy ions, (4) feasibility of indirect drive targets for lasers, (5) cost reduction strategies for heavy ion drivers, (6) demonstration of higher overall laser driver efficiency, (7) tritium self-sufficiency in IFE reactors, (8) cavity clearing at IFE pulse repetition rates, (9) performance, reliability and lifetime of final laser optics, (10) viability of liquid metal film for first wall protection, (11) fabricability, reliability and lifetime of SiC composite structures, (12) validation of radiation shielding requirements, design tools, and nuclear data, (13) reliability and lifetime of laser and heavy ion drivers, (14) demonstration of large-scale non-linear optical laser driver architecture, (15) demonstration of cost effective KrF amplifiers, and (16) demonstration of low cost, high volume target production techniques. Quantitative evaluation and comparison of the two design options have been made with special focus on physics feasibility, engineering feasibility, economics, safety and environment, and research and development (R&D) requirements. Two key conclusions are made based on the overall evaluation analysis: (1) The heavy-ion driven reactors appear to have an overall advantage over laser-driven reactors; and (2) However, the differences in scores are not large and future results of R&D could change the overall ranking of the two IFE concepts.

1. Introduction

Two commercial central station electric power plants have been conceptually designed and analyzed in the Prometheus [1] study led by McDonnell Douglas Aerospace. These plants use inertial fusion energy (IFE) technologies by employing the latest advances in KrF excimer laser and heavy ion drivers. Both of these two drivers are integrated with an advanced reactor cavity concept to offer power plants with the highest level of safety assurance and a low level of environmental impact. Advanced thermal conversion systems are employed to yield high efficiency plants capable of high reliability and a high capacity factor. Current target technologies are extrapolated in both performance and manufacturing capabilities. Fuel cycle systems are built upon a solid foundation of existing technologies. The two IFE power plant designs represent a wealth of information to help assess and develop a strategy and technical plan for the development of commercial fusion power plants based on inertial confinement.

Corresponding author: M.A. Abdou, Mechanical, Aerospace and Nuclear Engineering Department, 43-133 Engrg. IV, University of California, Los Angeles, Los Angeles, California 90024-1597, USA.

In this paper, critical technical issues identified during the development of these two designs and the research and development needed to resolve them are presented. Each critical issue contains several key physics and engineering issues associated with the major reactor components and impacts key aspects of feasibility, safety, and the economics potential of IFE reactors. The critical issues identified in the study are:

1. Demonstration of Moderate Gain at Low Driver Energy
2. Feasibility of Direct Drive Targets
3. Feasibility of Indirect Drive Targets for Heavy Ions
4. Feasibility of Indirect Drive Targets for Lasers
5. Cost Reduction Strategies for Heavy Ion Drivers
6. Demonstration of Higher Overall Laser Driver Efficiency
7. Tritium Self Sufficiency in IFE Reactors
8. Cavity Clearing at IFE Pulse Repetition Rates
9. Performance, Reliability and Lifetime of Final Laser Optics
10. Viability of Liquid Metal Film for First Wall Protection
11. Fabricability, Reliability and Lifetime of SiC Composite Structures
12. Validation of Radiation Shielding Requirement, Design Tools and Nuclear Data
13. Reliability and Lifetime of Laser and Heavy Ion Drivers
14. Demonstration of Large-Scale Non-Linear Optical Laser Driver Architecture
15. Demonstration of Cost Effective KrF Amplifiers
16. Demonstration of Low Cost, High Volume Target Production Techniques

In general, the critical issues identified here are for the two reactor design concepts developed in the Prometheus study. However, many of the issues tend to be generic and independent of the specific selections made here. These critical issues are examined in Section 2.

Evaluation and comparison of the two design options have been performed to help assess IFE program goals. An evaluation methodology was developed based on five major areas of evaluation. These include: (1) Physics Feasibility; (2) Engineering Feasibility; (3) Economics; (4) Safety and Environment; and (5) Research and Development Requirements. Each category is quantified through a system described in Section 3. The results of the evaluation processes for the two laser- and heavy-ion-driven reactor concepts developed in the Prometheus study are also summarized. Although the methodology is discussed and applied here for comparing the two IFE designs, methodology framework is general enough to allow extension in the future for comparing other options, e.g., comparing inertial and magnetic fusion reactors.

1.1. System description

Both of the Prometheus IFE power plants were designed to supply a net power output of 1000 MWe. The key parameter lists for the two power plant designs are presented in Table 1. The laser driver is less efficient than the heavy ion driver in producing the required energy to the target, which raises the thermal power, gross electric power, and recirculating power requirements for the laser-driven plant. The nominal pulse rate is 5.65 Hz. The type and number of laser amplifiers are chosen to enable the achievement of a nominal plant availability of 79.4%. The cost of electricity for this laser-driven plant is estimated to be 72.0 mills/kWh expressed in 1991$.

The system efficiency for the heavy ion driver is higher in producing the required energy delivered to the target. This effect translates into a lower recirculating power requirement, small physical sizes, and lower capital costs in most cost accounts. The nominal pulse rate for the heavy ion plant is 3.54 Hz. The heavy ion driver has an advantage in inherent availability which raises the plant availability to 80.8%. The resultant cost of electricity is estimated to be 62.6 mills/kWh expressed in 1991$.

The power plant designs were based upon today's known technology and physics extrapolated some 20–30 years into the future. Safety and environmental attractiveness were key design requirements to enhance the public's perception of fusion. Technical credibility was stressed in order to gain acceptance of the fusion community. Innovative concepts were encouraged to help foster and nurture developmental areas which may enhance the overall economics of fusion.

A single type of reactor cavity concept was judged acceptable for serving both the laser and the heavy ion reactor power plants. To provide low activation and safety enhancement, SiC was chosen as the major structural material within the high radiation environment of the reactor cavity. The first wall is protected by a thin film of liquid lead which is evaporated by each microexplosion and is recondensed on the wall surface between explosions, thus providing protection and vacuum pumping. The first wall is constructed as tubular panels of porous composite SiC structure, which is cooled with liquid lead. Behind the first wall, a lithium oxide solid breeder is cooled with a low pressure, high temperature helium coolant. A low pressure

Table 1
Major design parameters and features of the Prometheus plants

Parameter	Prometheus-L	Prometheus-H
Net electric power (MWe)	972	999
Gross electric power (MWe)	1382	1189
Driver power (MWe)	349	137
Auxiliary power (MWe)	36	28
Cavity pumping power (MWe)	25	25
Total thermal cycle power (MWt)	3264	2780
Blanket loop power (MWt)	1782	1597
Wall protection loop power (MWt)	1267	1162
Usable driver waste heat (MWt)	193	N/A
Usable pumping waste heat (MWt)	22	21
Thermal conversion efficiency	42.3%	42.7%
Recirculating power fraction	30%	16%
Net system efficiency	31%	36%
Fusion power (MW)	2807	2543
Neutron power (MW)	2027	1818
Surface heating power (MW)	780	725
Thermal power (MWt)	3092	2797
Thermal power to shield (MWt)	43	38
Cavity radius (m)	5.0	4.5
Cavity height (m)	15.0	13.5
First wall protection/coolant media (in/out temp.,°C)	liquid lead 375/525	liquid lead 375/525
Breeder material	Li_2O pebbles	Li_2O pebbles
Structural material, wall and blanket	SiC	SiC
Blanket heat transfer media (in/out temp.,°C)	1.5 MPa helium 400/650	1.5 MPa helium 400/650
Cavity pressure (mTorr, Pb)	3.0	10
Neutron wall load, peak/ave (MW/m^2)	6.5/4.3	7.1/4.7
Energy multiplication factor	1.14	1.14
Tritium breeding ratio (TBR)	1.20	1.20
Target illumination scheme	direct drive, symmetric	indirect drive, two sided
Number of beams	60	18 in LINAC (12 MAIN + 6 in 2 prepulses)
Driver output energy (MJ)	4.0	7.8 (7.0 transmitted to target)
Overall driver efficiency (%)	6.5	20.6
Ion accelerated	N/A	lead
Charge state	N/A	+2
Final energy (GeV)	N/A	4.0
Type of accelerator	N/A	single beam LINAC
Type and number of KrF amplifiers	electric discharge, 960	N/A
Beam combining technique	Raman accumulators	N/A
Pulse compression technique	stimulated Brillouin scattering	N/A
Final beam transport efficiency (%)	100	90
Target gain	124	103
Target yield	497	719
Repetition rate (pps)	5.65	3.54
Plant availability (%)	79.4	80.8
Cost of electricity (mills/kWh, 1991$)	72.0	62.6

helium purge extracts the tritium generated in the breeder material. The tritium breeding ratio is 1.2. All the lead and helium coolant piping within the bulk shielding is a SiC low-activation material. The operational lives of the wall and the blanket are five and ten years, respectively. The peak to average neutron wall load is 6.5/4.3 and 7.1/4.7 for the laser and heavy ion reactors, respectively.

A cylindrical reactor cavity was selected to maximize the maintainability of the first wall and blanket while keeping a reasonable balance of peak to average neutron wall loading. A trade study was conducted to determine the proper cavity aspect ratio. Modular construction and support techniques were analyzed to assure development of a maintainable design. Detailed calculations were performed to determine the nuclear performance of the first wall, blanket and the shield. The bulk shield was analyzed for both a concrete and a composite shield of B_4C, Pb, SiC, Al, and H_2O. The composite shield was chosen to provide a lower and more predictable activation level. In the case of the laser, the beamlines are protected by shielding beyond the final optics. The heavy ion final focus coils are also protected by shielding.

An elevation view of both the Laser Driver Building and the Reactor Building is shown in Fig. 1. The Reactor Building is 86 m in diameter as determined by the length of the shielded beamlines. The Driver Building containing all the laser systems surrounds the Reactor Building. The laser driver option uses 960 electric discharge lasers to provide a highly reliable power amplifier system. Non linear optical laser elements provide the beam combining and compression functions to provide high quality beams to the target. The laser driver delivers 4.0 MJ of 250 nm wavelength energy in sixty beams symmetrically onto a 6 mm diameter target. The beams are combined and the beam quality is enhanced with Raman Accumulator cells with an 88% conversion efficiency. The beams are compressed with Stimulated Brillouin Scattering (SBS) cells. Optical delay switch yards maximize the utilization of the unused energy in the SBS to provide a proper prepulse shape for the target. The sixty beams pass through optical foci at neutron pinholes to minimize neutron activation in the driver building. The final two optical elements in each of the 60 beamlines are final focus mirrors to focus, turn and point the beams. A grazing incidence metal mirror (GIMM) is the final optical element which lies in the direct line of sight of the center of the cavity for each beamline. Innovative design and choice of materials offers the possibility of an increased life of plant for the GIMM in a high radiation environment. This is especially difficult as this component is only 20 meters from the center of the cavity. The residual vapor pressure of the lead in the cavity is in the range of 3 mTorr or less for the laser beams to propagate through the cavity to the target.

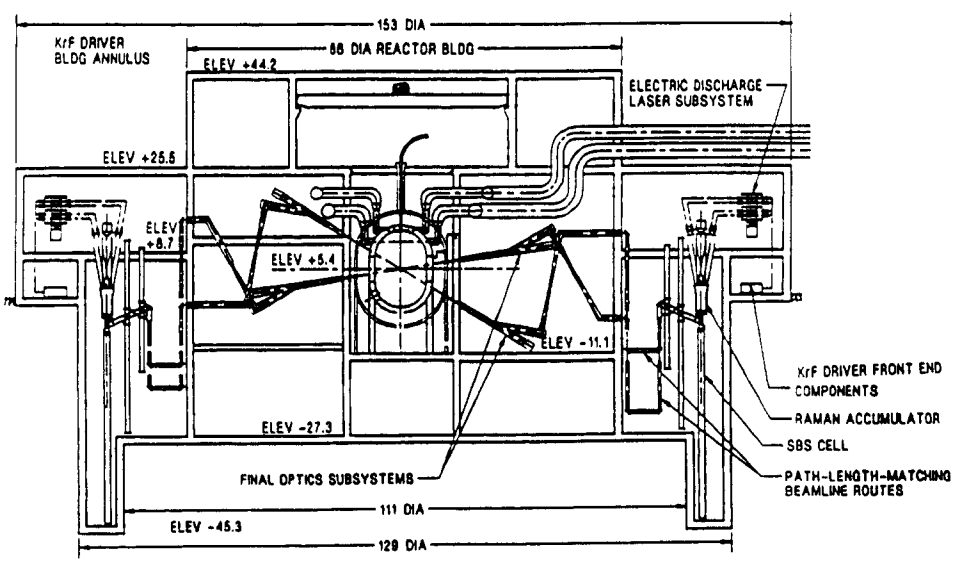

Fig. 1. Prometheus-L reactor building provides space for shielded beamlines. Driver building surrounds reactor building (all dimensions in meters).

An innovative design was chosen for the heavy ion driver. Heavy ion LINAC drivers have previously been thought to be very capital intensive, resulting in an unattractive cost of electricity. Several developments are being investigated to reduce the driver costs. The proposed design is a single beam LINAC which is rapidly pulsed a number of times. Eighteen beams are accelerated to 4 GeV and then are stored in storage rings for a time less than a millisecond. At the appropriate time, the beams are extracted and sent to bunchers to compress the beams. Six of the 18 beams are designated as prepulse beams to prepare the target for the remaining 12 beams. The beams are divided into two sets to be delivered to two sides of the reactor cavity for 2-sided target illumination. (A single-side heavy ion driver geometry was also developed). This final focus system is displayed in the elevation view of the heavy ion Reactor Building shown in Fig. 2. The main pulse beams are arranged in a 10° conical array with the precursor beams on axis. All beams are ballistically focused down to a focal spot size of 3 mm radius at the back of the blanket. The two precursor beams establish 3 mm radius, self-focused transport channels across the cavity to the target. This channel transport concept has the obvious advantage of minimal penetrations through the blanket, affording full and uninterrupted blanket coverage.

Two entirely different target concepts are used in the two studies. The laser driver is using a direct-drive, symmetrically-illuminated target with 60 beams. The direct-drivetarget capsule is roughly 6 mm in diameter. The beams are focused beyond the target to fully illuminate the target and provide a 1% illumination uniformity. The target is a CH plastic shell with beta-layered, solid DT on the interior surface. The gain of the target is expected to be 124. The direct drive target is protected with a sabot during the injection process with an electromagnetic injector. The target is separated from the sabot prior to passage into the reactor cavity.

The heavy ion, indirect-drive target uses a similar DT capsule, but it is enclosed in a radiation case. The case is cylindrical with an energy converter region in each end to convert the heavy ion energy into X-rays bathing the interior of the case and the DT capsule. The case has high-Z material (lead) to enhance the capture and distribution of the X-rays. The two heavy ion beams are focused on the two end energy convertor regions. The gain is expected to be 103. The indirect drive target is injected with a pneumatic injection system without the use of a sabot.

The energy conversion system used for both systems was chosen to be an advanced Rankine cycle. Two coolant streams, lead from the first wall and helium

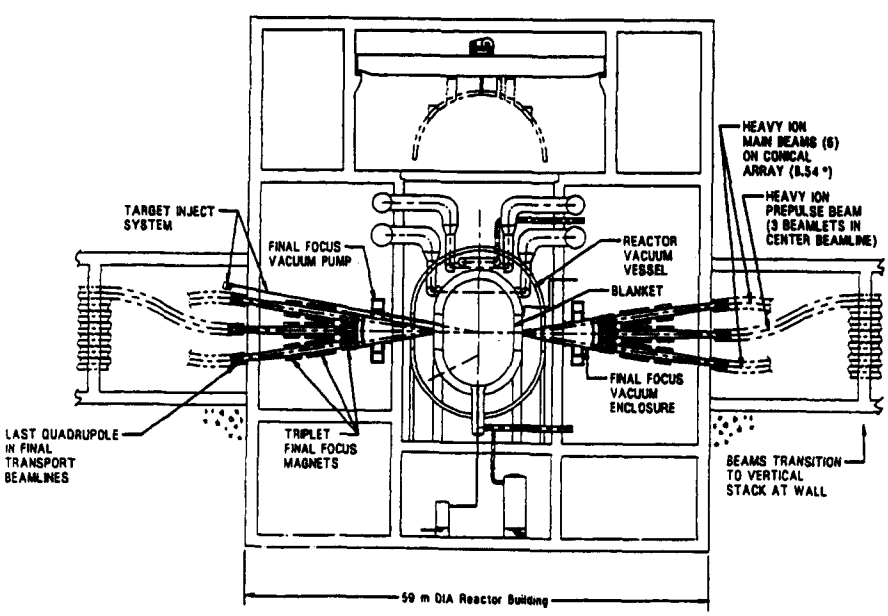

Fig. 2. Prometheus-H reactor building is relatively compact.

from the blanket are utilized. To improve the laser system efficiency, the waste heat from the KrF amplifier gas flow system is utilized in the energy conversion process. Steam-driven helium circulators are employed to minimize the power required to circulate the helium.

2. Prometheus reactor design study critical issues

Purpose

Although significant progress has been made in inertial fusion energy research during the past decades, the field is still in its early stage of research and development, and the present data base is severely limited. Therefore, many uncertainties exist in the actual performance and operation of present fusion reactor conceptual designs. The expected consequences of these uncertainties vary in magnitude: On one extreme, the uncertainties are so large that the feasibility of the reactor design is at stake, and, on the other extreme, the uncertainties may simply require moderate redesign, reduce performance, or increase cost. In viewing this, the study attempted to identify the key physics and engineering issues for the IFE conceptual reactor designs developed in Prometheus and determine the research and development (R&D) needed to resolve them.

In order to provide a brief summary of the most important issues, a smaller number of issues, called critical issues, were identified. A critical issue is broader in scope than a key issue; each critical issue may encompass several key issues. This section presents the critical issues for the two reactor design concepts developed in the Prometheus study. The major components and technical areas addressed are target, the laser and heavy ion drivers, vacuum system and evacuation, tritium processing system, reactor cavity, materials, safety and environment, balance-of-plant systems and subsystem interaction. Although some of the critical issues are specific to the Prometheus design concept, many of them tend to be generic and are fairly independent of the specific selections made here.

2.1. Critical issue 1: Demonstration of moderate gain at low driver energy

The U.S. National Energy Strategy [2] envisions three major facilities for IFE/ICF applications development: a Laboratory Microfusion Facility (LMF) for high gain target performance characterization and advanced military applications development; an Engineering Test Facility (ETF) to provide high pulse rate capability supporting fusion energy technology development and testing; and a Demonstration Power Plant (DPP) to validate long term economic, reliability, availability and maintainability issues for IFE. The total development cost associated with this plan will be formidable because each facility will likely cost more than $1B. It is therefore worthwhile to consider development paths that might enable a single facility to address both LMF and ETF research and development needs. Hogan discusses the prospects for such a facility in a recent paper [3]. Target experiments could be carried out in a separate, single-shot cavity. Engineering development would be conducted in another cavity with the target design and driver pulse rate selected to produce relatively low yield and fusion power. This approach would dramatically lower the cost of IFE development potentially leading to a more near-term DPP.

Reactor design studies have typically focused on high-gain, multi-megajoule incident energy target concepts that are appropriate for economic power production. However, engineering development, is usually cost limited. It therefore is worthwhile to consider if target designs that provide moderate gain (20–50) at low drive energy (1–2 MJ) are justified. Such targets would lower the facility cost associated with IFE engineering testing and fusion power demonstration. Target design studies for the Nova Upgrade have identified conditions under which the ignition "cliff" is shifted to much lower drive energy with the penalty of lower gain. This is illustrated in Fig. 3 which compares the projected gain for two different sets of implosion velocities and

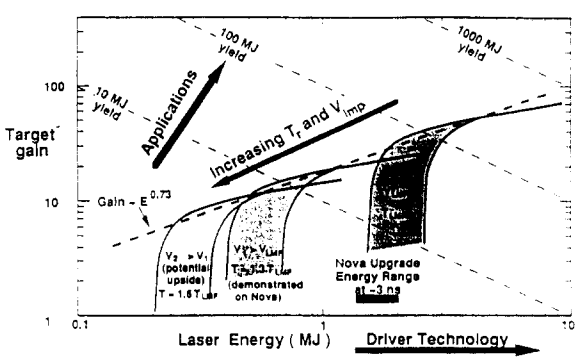

Fig. 3. Gain curve scaling with hohlraum temperature relative to gain for the LMF conditions. Nova upgrade will characterize the low energy (1–2 MJ) region of gain space and reveal how well the location and height of the ignition cliff can be controlled. (Figure Courtesy LLNL).

associated hohlraum temperatures to that projected for the LMF conditions. (The shaded region at the low energy end of the curves represents the uncertainty in the location of the ignition "cliff" due to uncertainty in the capsule surface finish).

As indicated, the alternative target designs coupled with a driver comparable to the Nova upgrade (1–2 MJ) would be above the ignition cliff and repeatably produce the output distribution (neutron/debris/x-ray split) and energy spectra of higher gain targets. Reactor component development testing could thereby be conducted at low drive energy with a cavity radius scaled appropriately to duplicate the relevant reactor parameters. In principle, this should provide the capability to achieve most of the ETF goals at relatively low power levels with full thermonuclear effects in a moderate cost facility.

Issue Resolution Strategy – To help identify the region of gain space that is attractive for reducing IFE development costs, the Prometheus driver, reactor and balance-of-plant design/cost scaling relations were used to project curves of target gain versus driver energy for a fixed capital cost facility. A 100 MWe demonstration power plant was chosen for illustration purposes. The costs are for a first-of-a-kind plant and include only direct construction costs. A summary of the cost elements included in the study and their scaling with yield (Y in MJ), pulse repetition rate (RR in pps), thermal power (P_{th} in MW), recirculating and gross powers (P_r and P_g in MWe) and driver energy (E_d in MJ) is presented in Table 2.

Table 2
Summary of Demonstration Power Plant direct cost scaling used in required gain curve study

Cost element	Cost scaling relationship (M$)
KrF laser driver (NLO)	$113+163\,E_d$
Single-beam LINAC (4 GeV)	$288+76\,E_d$
Multiple-beam LINAC (4 GeV)	$292+117\,E_d$
Single-beam LINAC (2 GeV)	$218+35\,E_d$
Multiple-beam LINAC (2 GeV)	$244+116\,E_d$
Land and structures	$60+150(P_f/500)^{0.3}$
Reactor plant	$50+480(P_{th}/3000)^{0.5}$ $+320(Y/500)^{0.5}$
Turbine plant	$13+176(P_g/1000)^{0.8}$ $+20(P_{th}/2860)$ $+59((P_{th}-P_g)/1860)^{0.8}$
Electric plant	$71.5+67(P_g/1000)$
Miscellaneous plant	$57(P_n/1000)^{0.3}$
Target factory	$50+100(RR/5.6)^{0.7}$

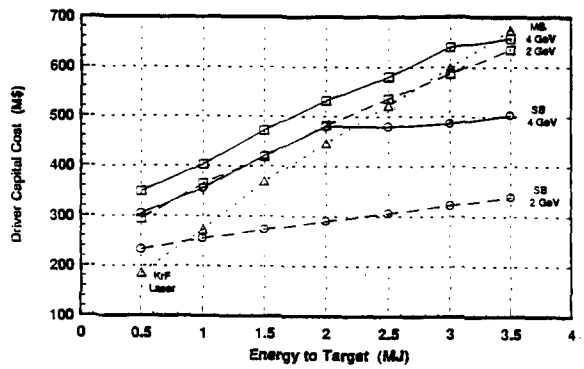

Fig. 4. Projected cost scaling for small-sized KrF laser and heavy-ion LINAC drivers.

The resulting driver cost variation with output energy is shown in Fig. 4 over the energy range of interest. This figure shows that projected laser costs are typically less than those for a multiple-beam LINAC but more than those for the 2 GeV single-beam system. The multiple-beam LINAC efficiency, however, is much higher than that for the other two driver options which offsets its higher cost.

Efficiency plays a key role in minimizing the reactor and balance of plant costs for small plants where the net power is comparable to that required by the driver. This is because the recirculating power is equal to $P_{th}/(M\,\eta_d G)$ where M is the blanket energy multiplication (1.1–1.4). If the recirculating power exceeds the gross power ($\eta_{th}P_{th}$), no net power is generated. Conversely, if $M\,\eta_d G$ exceeds $1/\nu_{th}$ by more than a factor of two, the reactor and balance-of-plant costs are determined primarily by the net power requirement. As a result, in a cost-limited scenario, the gain (hence yield

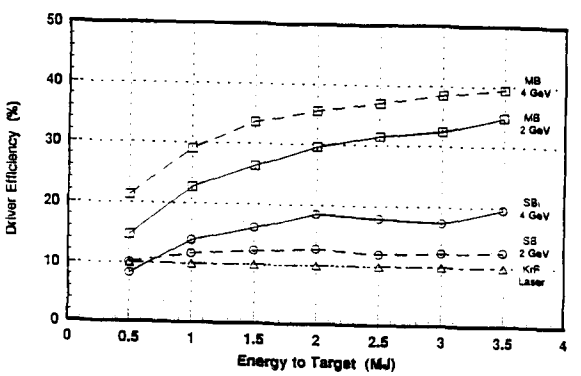

Fig. 5. Projected efficiency scaling for small-sized KrF laser and heavy-ion LINAC drivers.

and associated plant cost) required to produce net power scales directly with driver efficiency. Figure 5 shows the projected efficiencies for the drivers considered in this study. The 10% Prometheus-L system efficiency may ultimately be increased to 15%, but both values are well below the 30% efficiency possible with a multiple beam (MB) LINAC. This makes the MB LINAC an attractive option in spite of its higher capital cost.

It is also worthwhile to note that as driver energy increases, there eventually is no gain which will support both the recirculating and net output power requirements in a fixed-cost facility. The driver portion of the cost becomes too large. The required gain curves thus asymptote to infinity at some driver energy which is a function of the specified capital cost.

These simple power balance and cost relations were used to define curves of required gain versus driver output energy for different fixed direct capital costs. Figure 6 shows the result for a 100 MWe power plant based on the Prometheus-L driver design at 10 and 15% efficiency. It should be noted that the target design windows for cost-limited development are the important consideration here not the projected capital costs. Absolute costs may change, but the parametric scaling should result in similar design windows. To assess whether the design windows are feasible, Figure 6 compares the gain requirement curves to possible optimistic and pessimistic physics limitations on target gain for indirect-drive targets suggested by Hogan [4].

The figure shows that target gains of 30–50 at a drive energy of 1–2 MJ provide a possible DPP design window for either 10 or 15% laser efficiency. Improved efficiency enlarges the design window (or conversely

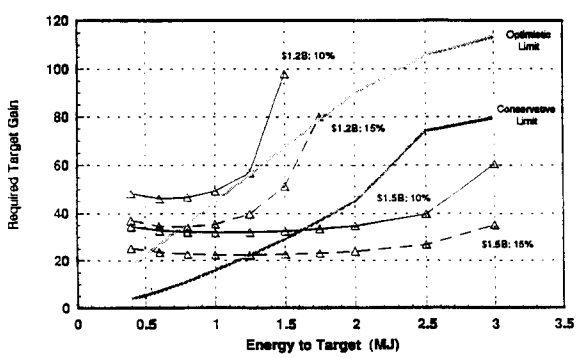

Fig. 6. Projected 100 MWe demonstration power plant gain space windows for the Prometheus-L driver configuration. Values indicated only include direct costs.

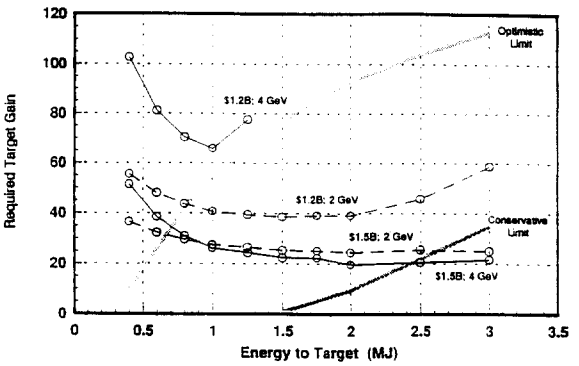

Fig. 7. Projected 100 MWe demonstration power plant gain space windows for the Prometheus-H driver configuration. Values indicated only include direct costs.

reduces the cost). But the gain required for a 10% efficient laser is less than conservative limits on possible target gain, with only $300M in additional funding beyond that needed to provide any design window. Therefore, there is significant motivation to develop target designs appropriate for this region of gain space. This is reinforced by the fact that such designs could likely be validated on Nova Upgrade.

The simple power balance and cost relations were also used to evaluate the gain space appropriate for heavy-ion drivers. Figure 7 shows these results for a comparable 100 MWe power plant with a single-beam (SB) LINAC driver based on the Prometheus-H design configuration. To assess the feasibility of such designs, Figure 7 again includes possible optimistic and conservative limits on gain suggested by Hogan [4]. This figure shows that SB LINAC power plants only require gains of 20–30 at a drive energy of 1–2 MJ due to the higher driver efficiency. This is greater than the conservative limit on gain scaling would suggest, but it is well below the optimistic gain scaling limit. A driver with 2.5 MJ output is required to surpass possible conservative limits on gain.

It is also worthwhile to note that the 2 GeV option may provide an extremely attractive development path. As indicated in Fig. 4, this driver costs ~ 60% of the 4 GeV system because it is half as long. At driver energies above 3 MJ, the number of beams becomes excessively large (greater than 40) for a 2 GeV system. However, if viable target designs are possible in the 1–2 MJ energy range, this option provides a very low-cost driver (< $300M) with a number of beams comparable to that proposed for the Prometheus-H power plant. Further characterization of heavy-ion tar-

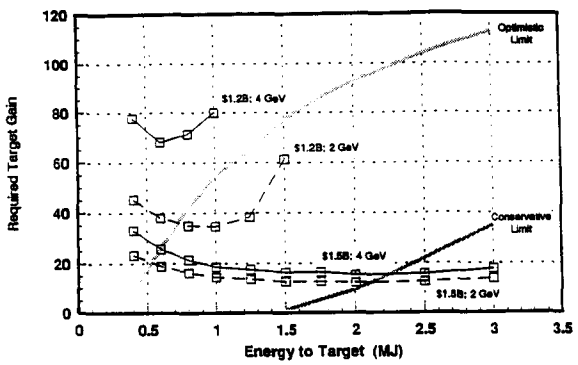

Fig. 8. Projected 100 MWe demonstration power plant gain space windows for a multiple beam LINAC driver. Values indicated only include direct costs.

get designs in this region of gain space thus is clearly justified.

Figure 8 shows these same gain space design windows for a 100 MWe power plant with an MB LINAC driver. This option eliminates the core recycling and storage rings required for the single beam design, which leads to efficiencies between 20 and 40% as indicated in Fig. 5. This makes the MB LINAC an attractive option for a DPP in spite of its higher capital cost, as indicated in Fig. 4, since recirculating power is significantly lower. This is highlighted in Fig. 8, which shows that the required gain curves for an MB LINAC are actually lower than those for the SBL once funding is large enough to get over the hump of its higher capital cost. Gains of 10–20 at driver energies between 1 and 2 MJ are all that is required to build a small DPP using an MB LINAC driver.

The figure also shows that the 2 GeV design may once again offer an attractive development pathway. The cost advantage of a 2 GeV system is reduced for the MB LINAC driver, as indicated in Figure 4, but its efficiency is comparable to that at 4 GeV. Furthermore, target performance will likely be improved at this energy because of the shorter ion range. A 2 GeV MB LINAC may therefore prove to be the best option for a heavy ion DPP. The SBL capital cost is significantly lower, but this is offset by reduced BOP costs for the higher MB LINAC efficiency for a small DPP where there is little excess ηG.

It, therefore, is critical that the Nova upgrade be implemented in a timely manner. Target experiments could then be conducted to characterize the location of the ignition cliff and the height of the gain curves for advanced target designs. This will establish a database for designing the ETF/LMF facility. An early ~2000 demonstration of low drive energy (1–2 MJ) target designs with repeatable gains comparable to those projected by this study would also provide strong justification for a lower-cost IFE development pathway utilizing such moderate-gain targets. This could provide the impetus to accelerate the engineering development and commercialization of IFE technology.

2.2. Critical issue no. 2: Feasibility of direct drive targets

Description of the problem – There are strong incentives to consider direct-drive (DD) targets because of higher gains. However, the feasibility and performance characteristics of DD targets are presently uncertain. The fundamental driver architecture of the Prometheus IFE Reactor Design is strongly influenced by the direct-drive (DD) target illumination requirements given by the project Target Working Group (TWG) *. Unfortunately, the specified TWG requirements may contain some serious inconsistencies with published plasma physics requirements for efficient laser/target coupling. The laser driver spatial intensity profile in the target plane provided by the TWG is not consistent with the Fresnel number of the beam at the location of the target. In addition, there are concerns that the long, 80 ns precursor pulse may produce significant deleterious effects, such as generation of non-linear scattering processes which may lead to target preheat, thereby preventing an efficient DT implosion from occurring. Designs for DD targets appear to have been anchored on experiments conducted on miniature DD targets illuminated with only a few kJ of laser energy. Large reactor sized, multi-MJ DD targets apparently require entirely different illumination scenarios. For reactor operation, the DD targets must also be accurately injected into the target chamber with a tracking/alignment system capable of meeting the illumination uniformity requirements set forth below.

Review of target illumination requirements supplied by TWG – The TWG has provided direct drive target illumination requirements which include the following elements:

(1) >60 beam illumination with $\pm 1\%$ illumination homogeneity of a 6-mm diameter target,
(2) 80 ns precursor pulse containing 30% of energy, followed by 6-ns main pulse (long prepulse generates underdense plasma atmosphere 3.2 cm deep prior to arrival of main pulse, thereby risking gen-

* The Target Working Group consists of senior individuals advising the Prometheus study (see ref. [1]).

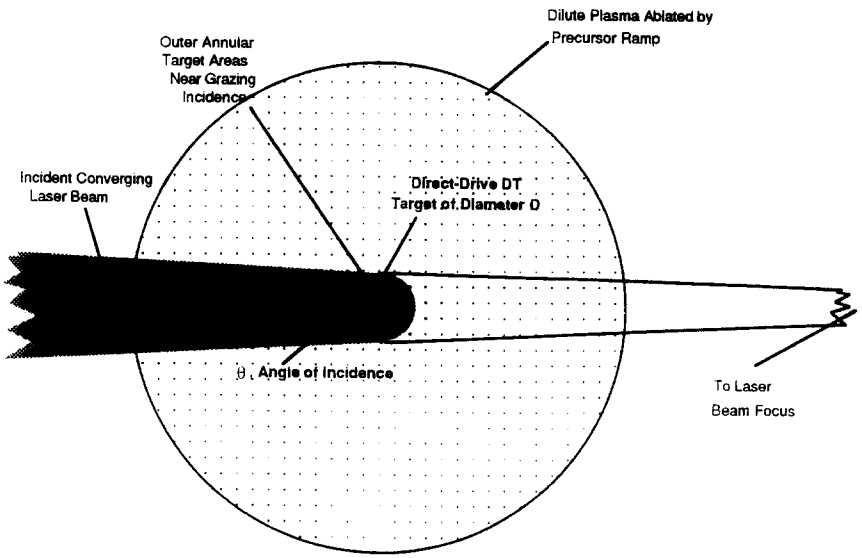

Fig. 9. Diagram of tangential direct-drive target illumination geometry at start of main pulse.

erations of SBS, Stimulated Raman Scattering (SRS), hot electrons, and resonant absorption mechanisms)

(3) UV wavelength (< 300 nm) with approximately 5 MJ of energy,

(4) Tangential illumination (beam diameter at target = target diameter); no mention of focal zoom; beams are circular in cross-section, (very wasteful of laser light, excimer laser beams are square, may encourage resonant absorption in underdense plasmas)

(5) The spatial intensity distribution of the incident

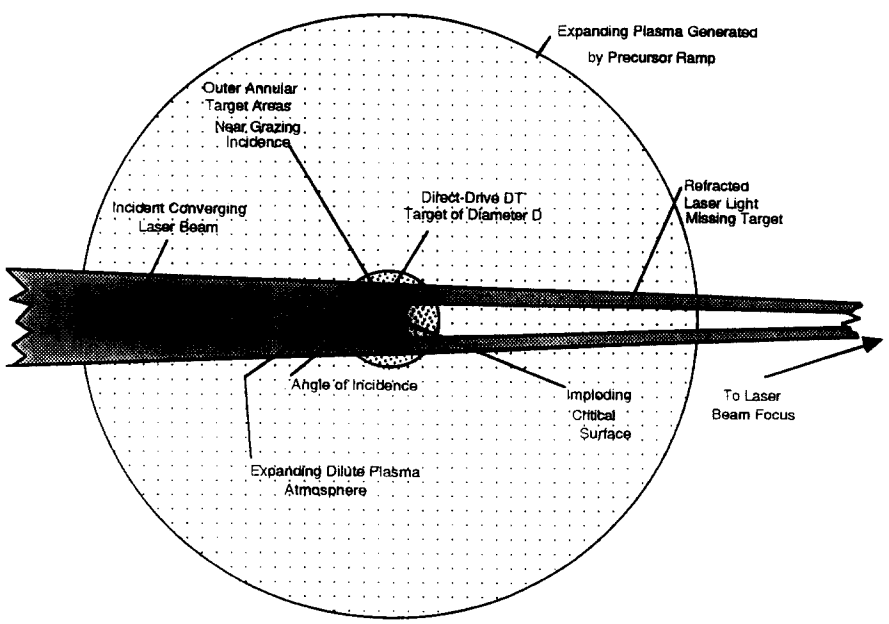

Fig. 10. Diagram of tangential laser illumination geometry at end of 6 ns laser pulse.

laser beams in the target plane is described by $I_{target}(x) = (\sin^2 x)/x^2$ (inappropriate apodization for homogeneous illumination and efficient excimer laser extraction)

There were, however, no TWG specified requirements on beam polarization, bandwidth, or beam quality, all of which are important parameters in laser/target interactions. During the 6 ns main pulse duration, the direct drive (DD) target implodes from an initial 6 mm diameter down to 3 mm, which corresponds to an implosion speed of 2.5×10^7 cm/s. Approximately 30% of the DT fuel is fused during the resulting implosion.

Physics of target implosion – Using the TWG criteria, the DD target is assumed to be a 6-mm CH spherical shell containing a layer of frozen DT. The initial laser photons incident on the CH shell blow off an underdense plasma from the CH shell to permit the main pulse to interact primarily with the plasma atmosphere. The intention is to drive a symmetrical implosion of the DT fuel to at least 20 times liquid density. A diagram of a single beam (one of many) tangentially illuminating a spherical direct-drive target at the start of the laser pulse is shown below in Fig. 9.

A precursor pulse this long produces an underdense atmosphere 3.2 cm deep by the arrival of the main pulse, thereby providing a long gain length for non-linear processes which can cause target pre-heat. During the resulting implosion occurring at a speed of approximately 2.5×10^7 cm/s, the target compresses to ~ 50% of its original diameter. Unless the laser beam focal spot sizes are also reduced ("ZOOMED") by 50%, a significant amount of laser light would consequently miss the target. A diagram illustrating this problem is shown in Fig. 10.

Recapitulation of published plasma physics target coupling requirements – Uniformity of target illumination for multiple beam geometries is essential for preventing the growth of Rayleigh–Taylor instabilities. However, it is also important that the angle of incidence, q, between the incoming laser beams and the target be minimized in order to absorb the incident beam efficiently into the critically-dense plasma atmosphere blown off from the target. According to Kruer [5], the fractional absorption, f_A, for a linear plasma density profile is given by the expression:

$$f_A = 1 - \exp\left(-\frac{32 v_{ei} L}{15c}\cos^5\theta\right), \quad (1)$$

which, as indicated, depends upon $\cos^5 \theta$. Here, v_{ei} is the plasma collision frequency evaluated at the critical density, n_{crit}. In addition, since an obliquely incident optical wave reflects from the plasma at a lower density than the critical density, less collisional plasma is traversed by these waves, further decreasing the coupling fraction. Calculations were carried out using this absorption function using the geometry shown below in Figure 11. Using this geometry and Eq. (1), the target coupling efficiency was calculated assuming that $f_A = 1$ for $\theta = 0$ with a top hat apodization; the results are plotted below in Fig. 12.

For a linear density profile averaged over the implosion time, these simulations estimate that only 15% of the laser light incident on the target will be absorbed. Since the actual beam shapes from the excimer lasers are square, a further reduction in target absorption efficiency of $\pi/4$ occurs. For an exponential electron density profile in the plasma ($n_c = n_{crit} \exp(-z/L)$, the fractional absorption, f_A, is given by the expression:

$$f_A = 1 - \exp\left(-\frac{8 v_{ei} L}{3c}\cos^3\theta\right), \quad (2)$$

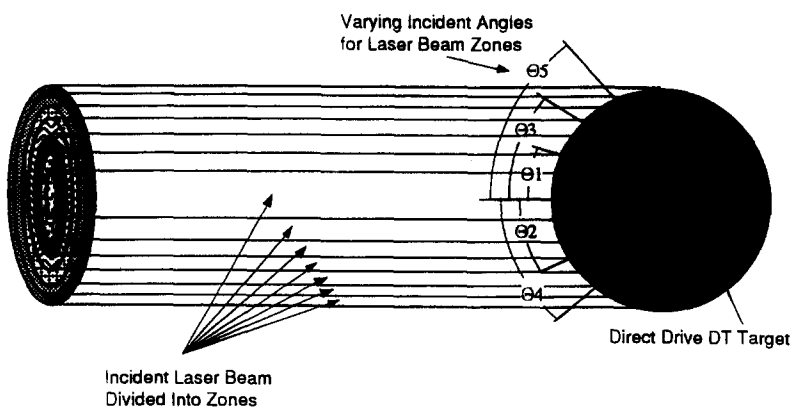

Fig. 11. Geometry for computing angular-dependent light/plasma coupling efficiencies.

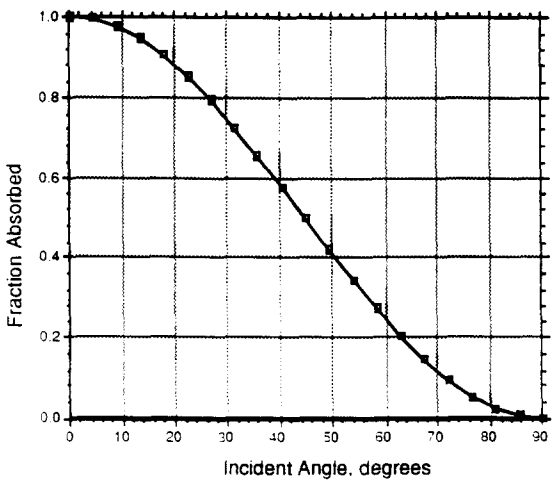

Fig. 12. Fraction of incident laser light absorbed for linear plasma density profile.

which, as indicated, depends upon $\cos^3\theta$. Calculations were also carried out using this absorption function with a top hat apodization. In this case, 28% of the energy incident on the target would be absorbed.

Resonance absorption calculations – The energy absorbed by resonantly driven fields in the plasma is described by the expression [6]:

$$E_{\mathrm{abs}} = \int \left(\frac{\upsilon(\langle E_r^* E_r \rangle)}{8\pi} \right) r^2 \, \mathrm{d}r \, \sin\theta \, \mathrm{d}\theta \, \mathrm{d}\phi, \tag{3}$$

where E_r is the radial electric field of the laser beam. Near the critical density, the expression for E_r is given by:

$$E_r = \frac{l(l+1)}{(\mathrm{i}\epsilon k^2 r^2)} a_l \left(1-\alpha_l^2\right)^{1/4} P_l^1(\cos\theta) \times \cos\phi \, \mathrm{e}^{\mathrm{i}\delta} \frac{\Phi^2(\tau_l)}{2\pi\gamma\alpha_l^2}, \tag{4}$$

where α_l is given by the expression:

$$\alpha_l = \frac{\sqrt{l(l+1)}}{kR_c}, \tag{5}$$

(where R_c is the radius of the plasma critical density) and where $\Phi^2(\tau_l)$ is the absorption function for the lth mode. The fraction absorption of the lth mode, f_{RA}, is given by:

$$f_{\mathrm{RA}} = \frac{\Phi^2(\tau_l)}{2\pi} \sqrt{1-\alpha_l^2}, \tag{6}$$

so that the total power absorbed from the laser beam as a consequence of resonance absorption is given by:

$$P_{\mathrm{RA}} = \sum_l \frac{P_l}{2\pi} \Phi^2(\tau_l) \sqrt{1-\alpha_l^2}, \tag{7}$$

where P_l is the laser power in the lth mode. The net result of performing the integral in Eq. (3) is to show that resonance absorption generally depends upon

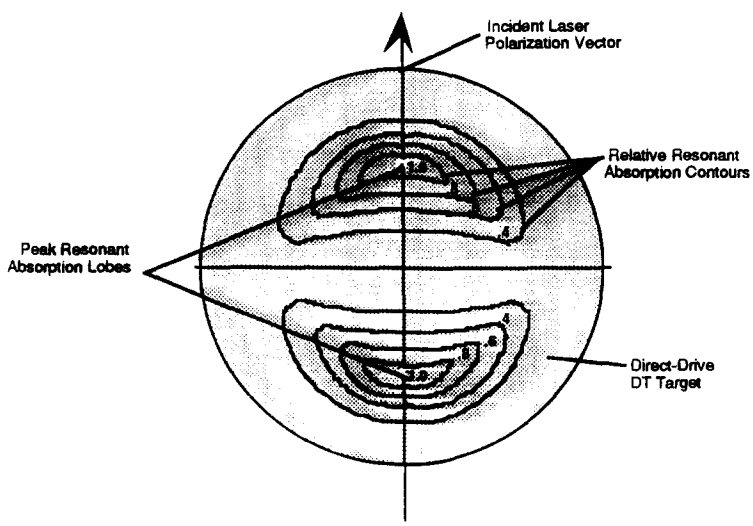

Fig. 13. Resonant absorption contours on spherical DD target.

(cos θ_0) [6]; the implication is that tangential target illumination proposed by the TWG would favor resonant absorption over inverse Bremsstrahlung for large angles of incidence. Perhaps a more serious result of these analyses [6] is that the spatial absorption distribution function is not uniform over the target sphere. The calculated RA distribution for a vertically polarized laser beam is shown in Fig. 13.

As shown, resonance absorption is predicted to produce two symmetrical "hot spots" of absorption at mid-latitudes on the sphere when illuminated with linearly polarized light. This may constitute an absorption uniformity problem because this process occurs even when the sphere is uniformly illuminated. However, by using $\lambda = 248$ nm laser radiation, the deleterious effects of resonance absorption are expected to be reduced relative to inverse Bremsstrahlung.

DD target injection, tracking, and alignment problems – The 6-mm DD target is assumed to be injected into the target chamber with speeds of the order of 200 m/s. Owing to the vagaries of mechanical and/or electromagnetic injection methods, tracking of the target and alignment of the 60 beamlines to the anticipated location of the target is mandatory. If tangential illumination is used, beams need to be aligned with an accuracy of $\pm 500\ \mu$ (corresponding to an angle $\Delta\alpha = 25$ mrad as seen by the GIMM) relative to the target. If pyramidal apodization is used, much more accurate target alignment is required (estimated to be $\pm 5\ \mu$ [corresponding to an angle $\Delta\alpha = 0.25$ mrad as seen by the GIMM]). In order to achieve the requisite alignment accuracy in this case, a reflective "shine shield" on the direct drive target is strongly recommended. Although DD target injection, tracking, and alignment present technological challenges, it is believed that these problems can be solved using careful engineering, parallel dedicated computer processing, and advanced metrology techniques.

Summary – Present specifications for the DD target illumination requirements such as those provided by the TWG, are based upon work performed at only a few kJ of laser energy. Elementary plasma physics and optics calculations suggest that the current TWG DD target illumination specifications are seriously flawed. It is essential that DD target results obtained at hundreds of kilojoules to megajoules be carried out as soon as possible to permit realistic DD target driver requirements to be generated. Such experiments could be performed using the Nova Upgrade laser proposed to be built at the Lawrence Livermore National Laboratory [7,8]. Using advances in laser technology together with SDIO tracking technology, it is anticipated that high gain DD targets could be developed which require only a few MJ of laser energy to achieve optimum performance. These large reductions in the requirements for laser energy can lead to significant reductions in COE as well as an increase in reliability. More importantly, the development steps will have facilities of much smaller size and moderate costs.

2.3. Critical issue no. 3: Feasibility of indirect drive targets for heavy ions

Description of the problem – The feasibility of the indirect drive (ID) targets for the heavy (HI) ion driver is, in part, linked to: (1) the properties of the method used to transport and focus the HI beam to the target, (2) the accuracy and reproducibility of the repetitive HI target launch system which injects the ID targets to the center of the target chamber, and (3) the ability of the high-Z hohlraum cavity to efficiently convert and smooth the radiation incident on the DT capsule. This study is involved with finding innovative solutions only to the first and second tasks.

In the approach being investigated for the Prometheus-H IFE Reactor Design, a number of HI beams are focused onto a stripping foil or cell placed in front of a pre-ionized channel. The HI beam(s) are then completely stripped, yielding mega-ampere currents which overcome space charge repulsion to self-focus the beam(s), thereby trapping the ions in a small diameter (a few mm) channel whose direction is accurately determined by the pre-ionizing beam. This self-focused, small diameter beam is subsequently directed to the convertor regions of the moving hohlraum target capsule. The target has been injected to arrive at the center of the reactor target chamber synchronously with the arrival of the HI beam(s).

Two types of indirect drive, heavy ion fusion targets were considered:

(1) Single energy convertor ID hohlraum targets designed for single-sided target irradiation (SSTI), and
(2) Dual energy convertor ID hohlraum targets designed for dual-sided irradiation (DSTI).

The feasibility of efficiently imploding both of these ID targets depends upon the solution of a series of technical problems, including:

(1) Providing return paths for the 13.3×10^6 A current for the SSTI beam and for 6.7×10^6 A for each beam for the DSTI case.
(2) Successful injection and self-pinching of the HI beams passing through the stripping foil(s) into a

self-focused, small diameter beam directed at the SSTI or DSTI ID target.

(3) Accurate pointing of the pre-ionized channel(s) at the energy convertor(s) of the ID target.

(4) Precise launching of the HI ID targets to arrive repeatedly at the center of the target chamber and synchronized with the arrival of heavy ion beams.

Review of target irradiation requirements supplied by TWG – The TWG has supplied the project with several unclassified documents [9,10] which were used to design a suitable HI driver design. The following general HI driver requirements were determined from the TWG recommendations:

(1) Tightly focused HI beams containing approximately 5 MJ of energy are to be delivered in a main beam pulse duration of 6 ns,

(2) The incident HI beam diameters need to be $\leqslant 6$ mm at the $1/e^2$ points,

(3) The HI beams must intercept the convertor regions with an accuracy of ± 0.5 mm.

Physics of single-sided HI ID target irradiation – Key to both the HI ID target irradiation of both single-sided and double-sided targets for the Prometheus IFE reactor is the collapse of all the separate HI beams into a single, pre-ionized channel of small dimensions. In the Prometheus IFE reactor design concept, this feat is accomplished by focusing the separate, bunched beams with large quadrupole magnets down to a common focus coinciding with a thin stripping foil. A schematic of this configuration is shown in Fig. 14. Background gas is present to permit autoneutralization of the focusing beams. Immediately prior to the arrival of the bunched beams, a non-bunched, precursor HI beam is precisely directed through the foil to the predicted location of the HI target. The target moves approximately 10 mm while the beams cross the cavity. Care must be taken to avoid damaging the HI ID target with the non-bunched beam. A dilute gas (Pb vapor) at a pressure of ~ 100 millitorr is present in the target chamber. The non-bunched precursor HI beam forms an ionized channel in the dilute lead vapor from the foil to the HI target.

Following the arrival of the bunched HI beams, each $+2$ ion is stripped to an $\sim +80$ charge state, thereby increasing the current to a level of approximately 6 MA. This beam current is more than an order of magnitude larger than is necessary to self-pinch the combined beams, thereby leading to a trapped, self-focused HI beam precisely directed to the energy convertor of the single-sided HI target. The diameter, d, of the self-pinched beam oscillates transverse to the beam direction with an amplitude determined by the original beam emittance and a period of approximately 20 cm.

Physics of double-sided HI ID target irradiation – The technical problems associated with double-sided HI ID target irradiation are similar to those described above for the single-sided HI ID target case. An additional constraint is that the two HI pulses must not

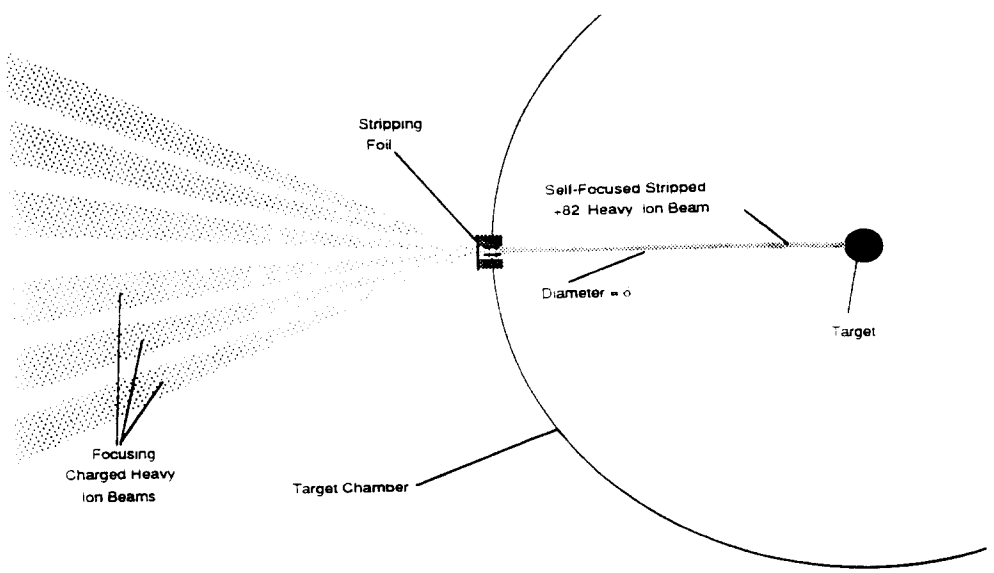

Fig. 14. Schematic of Prometheus approach for heavy ion single sided ID target irradiation.

only arrive near simultaneously at each of the target energy convertors, but they must also be accurately aligned spatially. A schematic of the double-sided HI ID target irradiation geometry is shown below in Fig. 15.

As noted above, key to the Prometheus HI ID double-sided target irradiation concept is the collapse of the two sets of separate HI beams into each of the two pre-ionized channels of $\leqslant 6$ mm diameter. In this case, the non-bunched precursor HI beams create the ionized channels in the low pressure (100 millitorr or less) lead vapor prior to the arrival of the HI ID target.

In a manner similar to that described above for single-sided irradiation, following the arrival of the $N/2$ bunched HI beams, each + 2 ion is stripped to a $\sim +80$ charge state, thereby increasing the current to a level of approximately 6 MA. This is sufficient to self-pinch the combined beams, thereby leading to a pair of colliding, self-focused HI beams precisely directed to the energy convertors of the double-sided HI target. Previous work performed with heavy-ion beams has shown that high degrees of precision can be achieved with regard to both timing of pulse arrival as well as intercepting a small aperture, providing the divergence associated with non-compensated space charge have been overcome.

ID HI target transport problems – The problems asociated with transport of the indirect drive heavy ion beam target relates to two general categories:

(1) Protection of the cryogenic target from thermal radiation, primarily emanating from the cooling interior of the reactor chamber,
(2) Accurate delivery of the indirect drive, heavy ion beam target to a location where the beams can successfully illuminate the target.

Indirect drive targets by their very nature are relatively fragile and difficult to accelerate rapidly. In general, accelerations greater than 100 m/s^2 are to be avoided. Target velocities should be in the range of 200 m/s to minimize the transit time across to the center of the chamber. Since the cryogenic DT capsule is relatively well protected from the thermal radiation present in the target chamber, the HI ID target is predicted to less prone to heating. Because of the 100 mtorr residual lead vapor pressure, the effect of viscous drag and turbulence on the motion of the target in the chamber must be determined.

Summary – In the Prometheus IFE reactor concept, the feasibility of indirect drive heavy ion targets is largely based upon the successful and efficient collapsing of a large number of low ionization state particles into one or two single, highly ionized, self-pinched ion beams that are accurately guided to the energy convertor(s) of a suitable heavy ion indirect drive hohlraum.

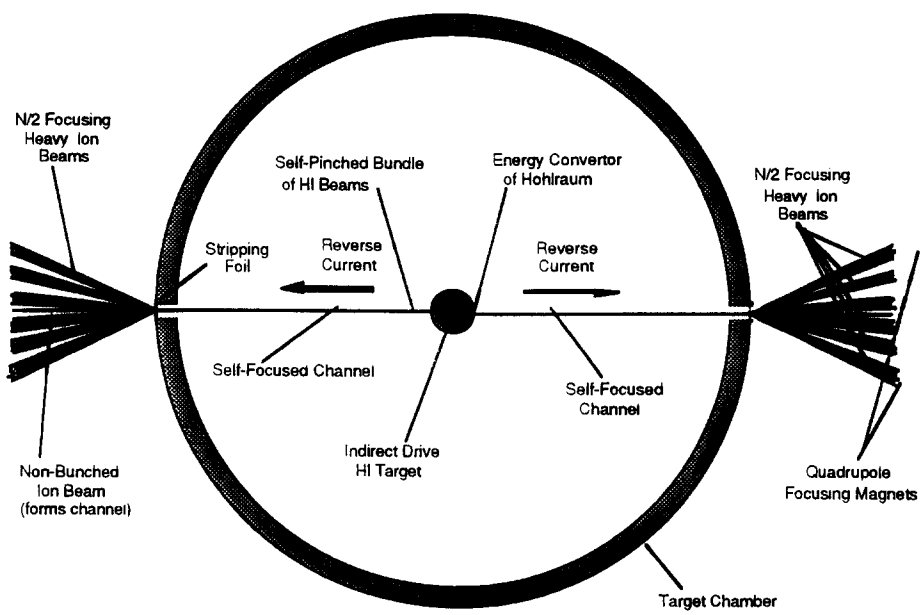

Fig. 15. Schematic of double-sided heavy ion ID target irradiation geometry.

Since the TWG specifications for HI ID targets were vague, the Prometheus IFE reactor concept has necessarily incorporated a great deal of flexibility in the final focus and transport portions of the heavy ion driver design.

It is important to demonstrate the validity of the Prometheus heavy ion final focus and self-pinched propagation physics experimentally. Since these experiments must be performed at full scale, it will be necessary to construct a substantial heavy ion driver machine in order to demonstrate the concept. It is strongly recommend that this be accomplished within the next decade.

2.4. Critical issue no. 4: Feasibility of indirect drive targets for lasers

Description of the problem – As in the case of the indirect drive heavy ion fusion target, the indirect drive (ID) laser fusion target being considered by the Prometheus IFE Reactor Design is a symmetric, two-sided hohlraum design. The feasibility of efficiently imploding this ID laser target has difficulties arising from three major sources:

(1) Plasma closure of the two entrance apertures to the hohlraum,
(2) Accurate target tracking and pointing of the multiple laser beams to coincide with the two entrance apertures of the moving ID target, and
(3) Accurate and reproducible indirect drive target propagation from the pellet injector to the center of the target chamber.

Significant misalignment of the laser beams could damage the radiation casing of the target capsule and cause a target misfire.

Review of target irradiation requirements supplied by TWG – As in the case of the heavy ion indirect drive targets, the Target Working Group (TWG) has supplied the team with unclassified documents. In the original inertial confinement fusion driver guideline document [9] supplied, all references to indirect drive laser targets had been removed. A second document [10], obtained much later, has some information concerning indirect drive laser targets. After careful examination of the information in these documents [9,10] from the TWG, the following laser driver requirements were surmised:

(1) Using the Nova Upgrade laser plan of 288 independently pointed beams arranged in three or four rings of beams on each side of the target with the beams distributed in angles ranging from 30° to 60° from the target axis, the indirect laser target illumination requirement is achieved. It should be possible to reduce the total number of beams to approximately 50. This would require an energy balance between beams of 5%. (Achieving a 5% balance of power among the laser beams is significantly easier than the 1% illumination uniformity required for direct drive laser targets)
(2) Nearly diffraction-limited laser beams are required with essentially all of the ~ 2.5 MJ in each of the two beams being contained inside a 1.5-mm diameter spot. Pulse durations range from around 8 ns at a 5 MJ energy level to 10 ns at 10 MJ of 6 ns. (This is readily achieved since the focal spot size from a 1-m aperture mirror located 20 m from the target chamber can achieve a 15-μm spot size).
(3) A laser wavelength is needed for which efficient inverse Bremsstrahlung can be achieved [UV Wavelength (< 300 nm)].
(4) A precursor laser pulse containing 30% of the energy and having a duration of 40 to 50 ns is required.

In general, these requirements are easier to meet than those specified for the laser direct-drive target. There are, however, some additional problems associated with ID laser targets which may seriously affect performance.

ID Laser target transport problems – As noted, indirect drive laser targets are relatively fragile and difficult to accelerate rapidly. In general, accelerations greater than 100 m/s^2 are to be avoided. Since the cryogenic DT capsule is relatively well protected from the thermal radiation present in the target chamber, the laser ID target can survive for longer periods in the target chamber (i.e., the propagation speed of the laser ID target need not be as great as that required for the laser direct drive target owing to this protective feature). See Section 2.3 for a list discussion of similar problems.

Summary – The feasibility of indirect drive laser targets is largely based on overcoming a number of potential technical problems: (1) directing 50 nearly diffraction limited laser beams accurately to the entrance apertures of the target and (2) reliably transporting the indirect drive target to the center of the target chamber with adequate precision. A great deal of flexibility in the final laser beam focus and transport portions of the laser architecture was incorporated to accommodate the range of specified requirements. As in the case of the direct drive target, technical development of high speed tracking and laser pointing systems are required in order to assure that all laser beams

would be properly positioned on the entrance apertures of the ID target.

2.5. Critical issue no. 5: Cost reduction strategies for heavy ion drivers

Description of the problem – The attraction of the Heavy Ion (HI) approach to IFE has always been related to the fundamental technical feasibility of building a system with the required properties to drive a pellet to ignition. The basic accelerator technology is well developed, the beam physics is tractable, and existing accelerator systems have exhibited 25-year lifetimes with 95% availabilities. A system to provide the required average power could have been built ten years ago. The problem is cost. A 10 GeV linear accelerator built with today's technology would cost billions of dollars. There are two key issues associated with HI driver cost reduction:

(1) Space charge limited transport of a bunched beam, and
(2) High current storage rings for heavy ion beams.

Each of these issues is briefly discussed below.

Space charge-limited transport of a bunched beam – Experiments and computer simulations have shown that transporting beams for several kilometers at their space charge limit should be possible, with little emittance growth. However, this HI beam transport has only been demonstrated with low energy, low power, unbunched beams.

If the HI beams have to be transported at currents lower than the space charge limit, then the accelerator will have to have a longer pulse (in the case of an induction LINAC) or more quadrupole transport channels within the same accelerator, thereby increasing the cost of the accelerator.

High current storage rings for heavy ion beams – One of the characteristic properties of linear accelerators is their ability to run at rather high average powers and relatively high repetition rates. Since the clearing time in the IFE reactor precludes very high repetition rates for the DT pellet ignition, the LINAC is forced to operate at uneconomical repetition rates. This problem can be eliminated if the beams for the LINAC can be stored for a short period of time. By operating the induction LINAC in the burst mode, the induction cores are used over and over, and of course, each core is therefore smaller in diameter.

The issue here is one of demonstrating that a HI beam of the required intensity can be stored in a storage ring for the requisite time, typically on the order of 1 to 2 ms. The issues are similar to those associated with bunched beam transport, but have the additional complications associated with closed orbit synchrotrons, such as betatron and synchrotron resonances, etc., which can give rise to emittance growth or beam loss. Furthermore, beam induced vacuum instability is another problem which must be overcome. All of these issues can only be resolved with an experimental ring with parameters reasonably close to what is required.

2.6. Critical issue no. 6: Demonstration of higher overall laser driver efficiency

Description of the problem – The excimer laser driver system has a number of components which can individually be optimized to yield high efficiencies. The achievement of high efficiency is viewed as a crucial requirement for the laser driver. In addition, however, to the achievement of high efficiency is the corresponding goal of highly reliable components. The Prometheus laser driver consists of the following four major elements:

(1) The excimer laser amplifiers,
(2) The Raman accumulators,
(3) The SBS pulse compressors, and
(4) The computer controlled and self-aligning optical train which directs the laser beams through the various optical components and down into the target chamber.

The latter three elements require some additional development and testing before they can be judged adequate to be incorporated into a mature laser driver design. The major problem to be addressed here is the first element, the excimer laser amplifiers. The fundament of an efficient, reliable Prometheus laser driver is the successful design, construction, and testing of excimer laser amplifier modules.

During the past five years, relatively little work has been carried out in the USA with regard to improving the efficiency and the reliability of moderate (~ 5 kJ) sized excimer laser amplifiers. Some analytical studies [11] have been carried out on both electron-beam excited excimer lasers (EBEELs) and electron-beam sustained electric discharge lasers (EBSEDLs) which offered (on paper) gross wall plug efficiencies as high as 17%. These efficiencies, however, are more likely to be reduced significantly if incorporated into a large laser system architecture. The main concern is that no experimental work in excimer amplifier development is

either currently in progress or planned by the Department of Energy (DOE).

Work in the former Soviet Union with sliding discharge cathodes in CO_2 discharge lasers has produced some promising results which may offer alternatives to the EBSEDLs. The electric discharge lasers offer an inherently higher efficiency than the EBEELs since excitation of the excimer species occurs along the neutral channel, thereby avoiding the excitation of a large number of higher-lying states (which may contribute relatively little to the overall amplifier extraction efficiency). Moreover, by avoiding transmitting large beam currents through foils, hibachis, etc., the overall pumping efficiency may be significantly higher.

Required future work on excimer laser amplifier modules – There are several problems with the electric discharge excimer lasers which require further experimental work. These include:

(1) Characterization of the optimum excitation pulse duration and gas mixture to achieve efficient operation with a matched, efficient, pulsed power system.
(2) Sensing and prevention of the formation of arcs in the discharges.
(3) Extension of the operating lifetimes of the amplifiers to reach levels of 10^9 to 10^{10} amplifier firings between failures.
(4) Control of color center formation and chemical attack of amplifier windows during the 10^9 to 10^{10} shot operational periods.

If these problems were analyzed theoretically and solutions found experimentally during a series of technological development programs granted by DOE to industry, the workhorse of the Prometheus excimer laser driver could be developed to the point that it could be incorporated into a believable IFE reactor system by the year 2030.

Summary – The major obstacle to the development of a reliable, highly efficient excimer laser driver for IFE reactors is the lack of work previously performed or currently planned on moderate-sized (2–6 kJ output) excimer laser amplifier modules. We strongly recommend that DOE support an aggressive excimer laser amplifier program with the goal of producing a 2 to 6 kJ amplifier with a wall plug efficiency of 12% and a mean time between failures of between 10^9 and 10^{10} shots.

Amplifier modules this size can fail in operation without producing a deleterious effect on the overall operation of the IFE reactor. Additional work would be needed on the Raman accumulators, SBS pulse compressors, and beam conditioning systems as well in order to achieve the objective of an efficient, reliable, operational IFE laser driver by the year 2030.

2.7. Critical issue no. 7: Tritium self-sufficiency in IFE reactors

Introduction – Fuel self sufficiency is a critical requirement for a renewable energy source. The first generation of fusion power reactors will operate on the DT cycle. Since tritium is not available in nature, tritium must be bred internally in fusion reactors using neutrons generated in the DT reactions. Therefore, careful analysis of the fuel cycle is necessary to evaluate the conditions that must be met in a fusion reactor design. These conditions must then be used as absolute criteria in selection among design concepts and in defining the range of acceptable performance parameters. Self sufficiency requirements must be included in a prudent plan for fusion research and development.

Several characteristics of tritium and fusion reactors that make fuel cycle analysis complex are (1) tritium is a gas in the natural state, (2) tritium undergoes radioactive decay with a relatively short half life, (3) tritium must be fed nearly continuously into the reaction chamber, (4) the fractional burnup, i.e. the fraction of the tritium atoms fed into the reaction region that undergo fusion reaction before they are removed out of the reaction region, is relatively low, (5) removal and processing of the fuel exhaust from the reaction region involve many physical, chemical and thermal processes and, generally, require a significant amount of time, (6) tritium bred in the blanket surrounding the reaction region must be extracted and processed through several processes that take time and, (7) the amount of tritium that can be produced in the blanket per fusion reaction is sensitive to the choices of particular technologies of key reactor components (e.g. neutral beams vs. rf in MFE or laser vs. heavy ion beams in IFE) and to many of the specific design features and performance parameters for a given technology (e.g. penetrations associated with direct or indirect KrF laser driver).

In previous work [12] fuel cycle analysis was performed and fuel self sufficiency conditions were derived for magnetic fusion reactors. There are substantial differences in the fuel cycle and in the reactor characteristics, and hence in fuel self sufficiency conditions and requirements between MFE and IFE reactors. The purposes of this work are (1) to develop a mathematical model for the fuel cycle in IFE reactors, and (2) to derive fuel self sufficiency conditions and requirements. Future work should compare the re-

quirements and potential for attaining self sufficiency in future IFE and MFE reactors.

Self sufficiency condition – The tritium breeding ratio (TBR), Λ is defined as [12]:

$$\Lambda = \dot{N}^{+}/\dot{N}^{-}, \tag{17}$$

where $\dot{N}^{+}$ is the rate of tritium production in the system (primarily, the blanket) and $\dot{N}^{-}$ is the rate of burning tritium in the fusion reaction chamber (i.e., the fuel target in IFE or the plasma in MFE). Defining two specific breeding ratios, the required TBR, Λ_r, and the achievable TBR, Λ_a; the condition to attain tritium self sufficiency in fusion reactors can then be written as:

$$\Lambda_a \geqslant \Lambda_r, \tag{18}$$

Since fusion is in a relatively early stage of R&D, accurate and clear definition of Λ_r and Λ_a must be general enough to account for uncertainties in reactor system description and in predicting its performance.

The required TBR (Λ_r) in a self-sustained fusion power economy must exceed unity by a margin, G, necessary to (a) compensate for losses and radioactive decay of tritium during the period between production and use, (b) supply a holdup inventory in various reactor components, and (c) provide inventory for startup of other fusion reactors.

The required Λ_r, as shown later, is a function of many reactor parameters as well as the doubling time, t_d, and the radioactive decay constant for tritium. Examples of these parameters are the fractional tritium burnup in the target, and the mean residence time and tritium inventory in various reactor components such as the target factory, blanket, and tritium processing systems. Many of these parameters vary from one de-

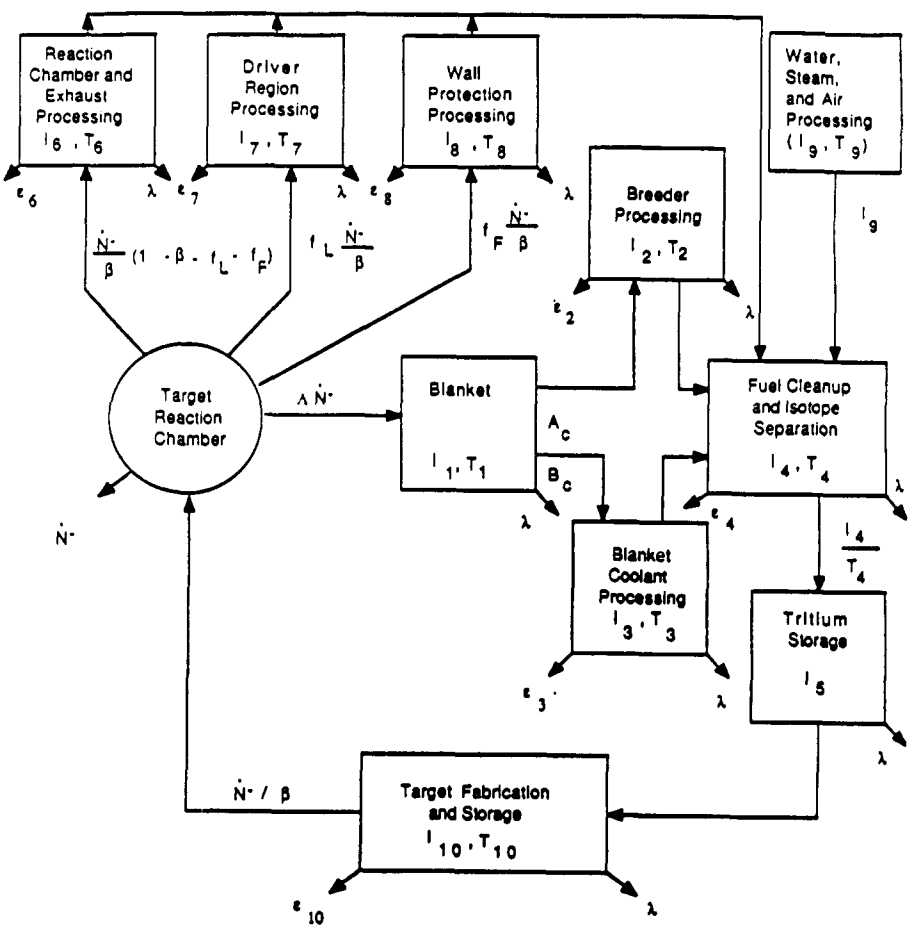

Fig. 16. Schematic model of the fuel cycle for IFE reactor operated on the DT cycle.

sign to another; and, for a given design, the prediction of some of these parameters is subject to uncertainties. We write:

$$\Lambda_r = 1 + G_o + \Delta G, \tag{19}$$

where G_o is the breeding margin for a reference conceptual design based on a given estimate of its performance parameters, and where ΔG is the uncertainty in estimating the required breeding ratio $(1 + G_o)$.

The achievable TBR, Λ_a, is also a function of the reactor design with particularly strong dependence on the first wall/blanket design concept. At present, accurate prediction of Λ_a suffers from two types of uncertainties:

1) Uncertainties in system definition: Fusion reactor design concepts are evolving. The choices for many of the design features, materials, and technology options have not been made. The achievable TBR is strongly dependent on many of these choices.
2) Inaccuracies in prediction: For a well-specified reactor system, the prediction of the achievable breeding ratio is subject to uncertainties. These are due to approximations or errors in the various elements of the calculations, e.g., in basic nuclear data, data representation, calculational methods, and geometric representation. We write the achievable TBR, Λ_a, as:

$$\Lambda_a = \Lambda_c - \Delta_a, \tag{20}$$

where Λ_c = TBR calculated for a specified blanket in a specified reactor system, and Δ_a = uncertainty in calculating the achievable TBR:

$$\Delta_a = \sqrt{\Delta_s^2 + \Delta_p^2}, \tag{21}$$

where Δ_s = uncertainty associated with system definition; i.e. the changes in Λ_c due to probable changes in the system definition, and Δ_p = uncertainty in predicting the breeding ratio (Λ_c) for the specified system due to nuclear data uncertainties, numerical approximations, geometrical modelling, etc.

In comparing the potential to achieve tritium self sufficiency among various reactor concepts or among various blanket options for a given reactor design, it is useful to define a "figure of merit." One such figure of merit is

$$\epsilon = \Lambda_a - \Lambda_c = (\Lambda_c - \Delta_a) - (1 + G_o + \Delta G), \tag{22}$$

Required TBR – The analytic model developed in ref. [12] was modified to describe the various elements of the tritium cycle in an IFE reactor. The model is shown schematically in Fig. 16. A set of differential equations was written down to relate the tritium inventories in the various components of Figure 16 to their operating parameters. The equations were solved analytically to derive explicit expressions for the functional dependence of the tritium inventories. An exact expression for the required TBR as a function of the doubling time and the tritium cycle operating parameters was derived. A computer program was written using these equations to calculate the dependence of the required TBR on the key physics and technology parameters of an IFE reactor. Table 3 denotes the abbreviations used in Fig. 16.

Table 3
Abbreviations used in Figure 17

Λ	= tritium breeding ratio
$\dot{N}$	= tritium burn rate in the target
l_i	= tritium inventory in compartment i
T_i	= mean residence time of tritium in compartment i
ϵ_i	= nonradioactive loss fraction of tritium in compartment i
λ	= tritium decay constant
β	= tritium fractional burnup in the target
f_i	= tritium fractional leakage to compartment i
l_g	= constant flow rate of tritium recovered from waste, steam, and air processing units
A_c	$= l_1 / T_1 (1 - f_c)$
B_c	$= l_1 / T_1 f_c$

A set of reference parameters was selected to represent the present best estimate. This reference parameter set is shown in Table 4. The calculated value of the required TBR with this reference parameter set is 1.05. A sensitivity study was then performed to determine the sensitivity of Λ_r to variations in various parameters. It was found that the required TBR is most sensitive to:

- β: tritium fractional burnup in the target,
- T_{10}: the tritium mean residence time in the target factory,
- t_r: the number of days of tritium reserve on site,
- t_d: the doubling time.

Figure 17 shows the variation of the required TBR with these most important parameters. It can be seen from this figure that the required TBR can increase to ~ 1.25. Figure 18 shows the variation of Λ_r with simultaneous change in the values of β and T_{10}. The required TBR increases dramatically, e.g. to ~ 1.5 if β drops to 5% and T_{10} becomes 20 days. Such high TBR can not be achieved in a fusion reactor.

The achievable TBR is generally in the range of 1.1 to 1.3 with about 20% uncertainty due to system definition and prediction capability. Two important conclusions arise from this analysis:

1. R&D effort for IFE must aim at achieving certain range of parameters that have direct impact on tritium self sufficiency. For example, the R&D goals should be to achieve $\beta > 20\%$ and $T_{10} < 10$ days.
2. Tritium self sufficiency is a critical issue in IFE, as it is in MFE. Demonstration of tritium self sufficiency must be a goal for early integrated test facilities.

2.8. Critical issue no. 8: Cavity clearing at IFE pulse repetition rates

Following each pellet explosion, the cavity fills with target debris and material evaporated or otherwise ejected from the cavity surfaces. This material must be removed from the cavity before the next target is injected. In the Prometheus designs, the cavity is cleared by recondensing the condensable gases onto the surface of the first wall, and by pumping non-condensible gases out through large ducts.

Operation of a power reactor requires continuous operation at several (i.e., ~5–10) pulses per second. For a fixed reactor thermal power, lower repetition rates require higher yields, which in turn produce unacceptably high driver energy requirements and excessive loads on the surrounding components. In order to ensure that a feasible design window exists, the cavity pressure must be reduced to the level required for target and driver energy propagation.

Evacuation requirements are based on propagation limits for both targets and driver energy. Base pressure requirements are important for two reasons: (1) the time to evacuate the chamber depends on the pressure, and (2) the level of protection to the first wall (and final optics) afforded by the cavity background gas depends strongly on the pressure. If a sufficiently high background pressure could be allowed, the survivability of the solid surfaces might be substantially enhanced.

Driver propagation requirements depend on the type of driver. For the Prometheus-L design, the Pb pressure limit for laser propagation was estimated as ~1 mTorr at 0°C. Above this value, gas breakdown is expected to occur, in which case the laser beams would be degraded. Target gain would start to decline.

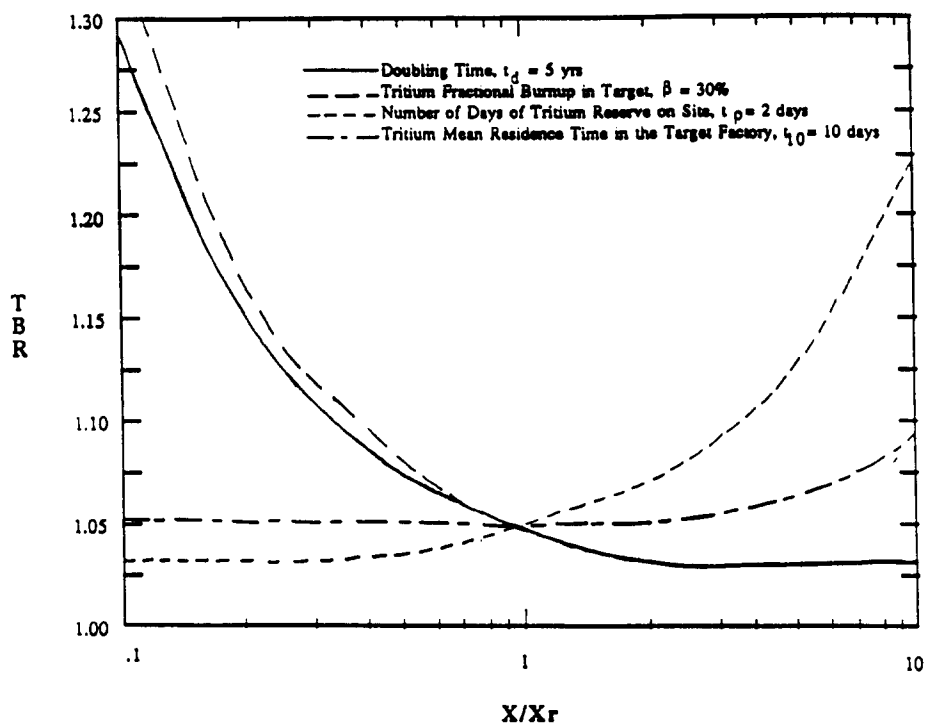

Fig. 17. Variation of required TBR with reactor parameters.

Table 4
Reference parameter set for tritium self-sufficiency calculation

Tritium consumption (burn in plasma), $\dot{N}^-$ (kg/day)	0.3
Doubling time, t_d(yr)	5
Tritium fractional burnup in plasma, β(%)	30
Time reserved for independent tritium supply, t_r(day)	2
Non radioactive losses (chemical tie-up in radioactive waste, etc.) in:	
Breeder processing, ϵ_2(%)	0.02
Blanket coolant processing, ϵ_3(%)	0.001
Fuel clean up and isotope separation units, ϵ_4(%)	0.0
Reactor chamber and exhaust processing, ϵ_6(%)	0.05
Driver region processing, ϵ_7(%)	0.1
Wall protection processing, ϵ_8(%)	0.1
Target fabrication processing, ϵ_{10}(%)	0.1
Tritium mean residence time in:	
Blanket, T_1(day)	1
Breeder processing, T_2(day)	0.1
Blanket coolant processing, T_3(day)	100
Fuel cleanup and isotope separation units, T_4(day)	1
Reaction chamber and exhaust processing, T_6(day)	1
Driver region processing, T_7(day)	100
Wall protection coolant processing, T_8(day)	100
Target fabrication and target storage, T_{10}(day)	10
Tritium fractional leakage from:	
Breeder to blanket coolant processing, f_c(%)	0.001
Plasma to limter processing, f_L(%)	0.01
Plasma to wall protection processing, f_F(%)	0.01
Constant tritium flow returned from the waste, steam and air processing, 19(g/day)	0.01

Due to the innovative, heavy-ion channel transport mechanism used in Prometheus-H, a much higher base pressure is considered acceptable. In this case, the 100

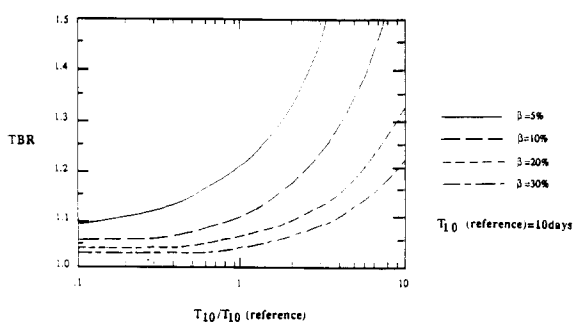

Fig. 18. Variation of required TBR as a function of T_{10} (residence time in target factory) for various values of the tritium fractional burnup (β).

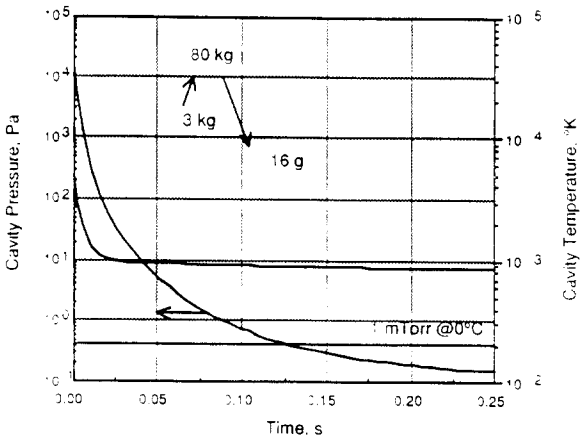

Fig. 19. Cavity vapor pressure and temperature histories following the blast.

mTorr limit is determined also by target transport. Target propagation limits depend on the target design. Indirect drive targets are generally more robust than direct drive, and can propagate at higher base pressure with less degradation. In order to resolve this aspect of the issue, accurate estimates of maximum allowable base pressure need to be determined for each target and driver design to be pursued.

Under idealized conditions, achievable cavity clearing times can be estimated by analyzing mass and energy transport within the cavity. Figure 19 shows the results of such a calculation. Cavity vapor temperature and pressure histories are plotted for a Pb wetted-wall cavity design. In this case, approximately 3 kg of Pb are evaporated by direct energy deposition from the X-rays which reach the first wall. The initial average cavity vapor pressure and temperature are estimated as 49 kPa and 3 eV, respectively. A much larger amount of Pb is subsequently evaporated due to rapid radiation cooling of the cavity vapor. Before the recondensation phase begins, about 80 kg of Pb (10 μm) is evaporated.

Based on this analysis, the cavity pressure drops below 1 mTorr before the next shot. However, the actual physics of energy and mass transport and vapor recondensation is very complex under the extreme conditions following a target explosion. The cavity gas is partially ionized, and subject to highly time-dependent processes such as hydrodynamic shock waves. Non-ideal effects such as liquid droplet formation and effects of penetrations provide additional uncertainties.

While many uncertainties exist, there are also various design solutions which can be adopted to improve the cavity clearing rate. For example, condensing sur-

faces (or cold jets) could be added. Some design proposals use large slugs of cold liquid to evacuate the chamber. More research is needed to better understand clearing requirements, the recondensation process, and to develop design solutions to this critical issue.

2.9. Critical issue no. 9: Performance, reliability, and lifetime of final laser optics

Description – In this study, successful conceptual mirror designs were introduced. These designs involved both the dielectric turning and focussing mirror and the final optical component; the Grazing Incidence Metal Mirror (GIMM). Analysis of the proposed design indicated that, with proper selection of materials and mechanical configuration, the GIMM lifetime can be very long – on the order of the plant lifetime. Clever shielding designs, and materials selection for the dielectric elements can likewise lead to great improvements in the overall laser reactor concept. In all previous studies of laser fusion so far, it has always been concluded that the the final mirror will have to be at distances in excess of 30–40 m away from the cavity center, and that the lifetime and reliability will be small. Preliminary analyses of the Prometheus design approach indicated the mirror could be a life-of-plant component and yet be located 20 meters from the cavity center. An in-depth study of the performance, reliability and lifetime of the final optical components is necessary. Advances in this area will undoubtedly lead to significant improvements of the entire concept, and will likely benefit other technological areas which rely on the reliable performance of large laser mirror systems.

Analysis

Turning mirror – As far as the turning mirror is concerned, two categories of research will be pursued:

(1) Shielding design of a neutron dump, and pinhole for minimization of the damage caused by ionizing radiation (i.e. neutronic and photonic).
(2) Materials selection and data base analysis for the optimum choice of dielectrics with the minimum amount of damage. In this area, rate theory would be used to compute the accumulation rates of color centers, and their impact on the optical properties of the dielectric. To our knowledge, this approach has not been attempted so far. A model with these capabilities can actually lead to the development of annealing strategies for the elimination or reduction of the effects of radiation on the optical properties of the dielectric materials.

Grazing Incidence Metal Mirror (GIMM) – The design of a reliable, long-life GIMM is critical to the success of the laser fusion concept. A detailed thermomechanical design involves the following features:

(1) Decoupling between the optical and structural functions of the mirror. A high strength aluminum alloy is deposited on top of a composite SiC stiffened support structure. A very thin graphitic shear layer would be desirable, such that the larger thermal expansion of the aluminum surface does not lead to buckling patterns on the mirror's surface which would degrade the optical quality of the laser beam.
(2) A low activation, zero swelling composite structural support of the aluminum surface. Thermal deformations of the surface are corrected by uniform end moments. These correcting moments can be induced by clamping the structural support to a rigid concrete shell, which would also give only one or two degrees of freedom for thermal expansion. Design of mechanical sliding/bolting systems must be demonstrated in order that the deflections caused by the small temperature gradient across the mirror's surface can be completely eliminated.
(3) Detailed structural analysis of the aluminum optical layer, the supporting composite structure, and the graphitic shear layer.
(4) Determination, and analysis of the possible modes of damage to the mirror. This would involve fatigue and creep damage assessments. It is to be borne in mind that fatigue analysis of the composite structural substrate does not follow the established rules for metal systems. On the other hand, fatigue of the surface aluminium layer (a few mm thick) can also be minimized, or perhaps eliminated, if more effort is directed towards stress redistribution in between the optical aluminum layer and the structural substrate.
(5) Investigation of the possibility of piezoelectric, or other error detection and correction mechanisms, for final mechanical control of the optical quality of the mirror's surface.

2.10. Critical issue no. 10: Viability of liquid metal film for first wall protection

In the Prometheus designs, a thin liquid metal film wets the first wall in order to prevent the solid structures from rapidly degrading due to the extremely high

instantaneous heat and particle loads. To prevent liquid from entering the cavity, the thickness of the film is maintained as small as possible. For this scheme to be successful, all structures exposed to the blast must be covered. Analysis of dry spots suggests that operation for periods of time greater than 10–15 minutes will cause irreparable damage to the first wall.

While a great deal of research has been carried out on film flows, the materials, configuration, and environmental conditions for fusion are unique, and little effort has been expended in the IFE community to determine how films will behave under these conditions in a real engineering system. The major uncertainties include:

- Film feeding and thickness control
- Blast effects
- Flow around geometric perturbations (such as beam penetrations)
- Protection of inverted surfaces.

The film thickness must be relatively uniform in Prometheus because the surface power conducts through the film. The local film thickness determines the local surface temperature, which strongly influences the condensation rate. Even for very thin films, the flow becomes turbulent and instabilities are likely to develop. Therefore, better understanding of the nature of instabilities and possible remedies are critical. Good wetting between the solid surface and liquid film is very important.

Explosive effects resulting from the blast may lead to further problems. Several effects are present:

(1) A large impulse is imparted to the film following rapid evaporation at the surface.
(2) Additional shock waves strike the wall as the cavity vapor responds to the blast. These shocks cause motion of the solid structures which could eject liquid into the chamber.
(3) Rapid "isochoric" bulk heating of the liquid creates high pressures, which can cause fragmentation of the liquid film.

The problem of wall protection with films is particularly difficult near inverted surfaces (such as the upper hemisphere or tops of beamlines) or at penetrations and nonuniformities in the cavity interior. Dripping is likely to occur from inverted surfaces, so that the concept of slow porous flow may need to be supplemented with alternate methods, such as inertial jets or magnetic guiding.

Figures 20 and 21 show the jet velocity required, and the film thickness and minimum flow rate required for film attachment on the upper hemisphere. The velocity and thickness can be high, leading to large flow rates. The option of using MHD guiding has been shown to be capable of resolving this problem, but adds design complexity to the device.

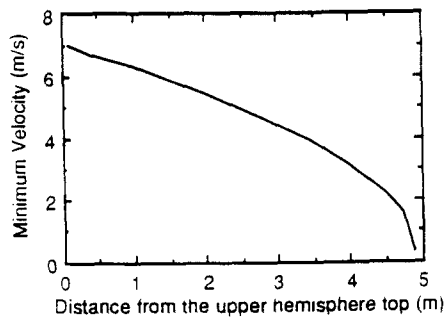

Fig. 20. Minimum velocity required for film attachment on the upper hemisphere.

2.11. Critical issue no. 11: Fabricability, reliability, and lifetime of SiC composite structures

Description – The viability of using SiC structures in the first wall and blanket is a key consideration of the laser and heavy ion designs. If these concepts are to be believable, efforts should be made to assess the factors involved in determination of acceptable lifetimes, and to determine the appropriate manufacturing methods and their economics. Anticipated lifetimes for FW/B components are not well known. Limited resources allocated to this area precluded a realistic assessment of the anticipated lifetimes. Without this knowledge, system reliability, maintenance and economics would be seriously challenged. In order to perform this task,

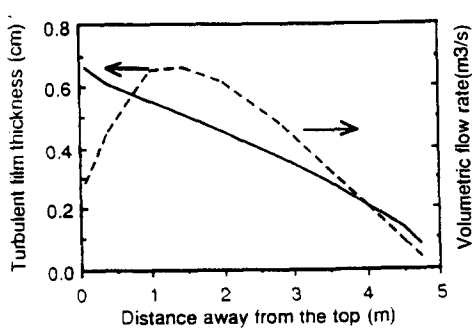

Fig. 21. Turbulent film thickness and minimum flow rate required for film attachment on the upper hemisphere.

several investigations need be considered. It is too simplistic, and perhaps misleading, to use the accumulated fluence, or displacements per atom, to make projections of lifetimes. The determination of such lifetimes would need knowledge of the various effects of radiation. The most prominent of those are neutron induced swelling, embrittlement, fiber shrinkage, and/or detachment from the matrix, creep crack propagation at high temperatures, and crack bridging mechanisms during irradiation.

On the other hand, the technology to process and manufacture SiC composites is in its infancy. An evaluation of manufacturing methods, potential, and costs is needed. Manufacturing methods are classified into fiber production techniques and matrix processing technologies. A variety of possibilities exist, with potential consequences on both economics and design.

Analysis

(1) Radiation effects on the properties of SiC composites: The relevant effect of irradiation to be investigated are: displacement damage production in various neutron spectra; swelling rate dependence on temperature, fluence and porosity; irradiation induced creep; irradiation embrittlement by amorphization; high temperature crack nucleation and propagation under static and dynamic conditions.

(2) Lifetime assessment of the FW: A realistic determination of FW lifetime would require analysis of a number of material and structural properties of the first wall. The data base accumulated under item (1) above would have to be phenomenalogically modeled in the form of appropriate design equations. These equations will include crack growth under cyclic loading at high temperature, radiation creep rate, thermal creep rate, and swelling rate. These mechanical property equations will then be used in a structural analysis code for determination of stress and strain fields under time-dependent loading conditions. The lifetime of the FW/B structure will be dictated by:

(a) fatigue crack growth,
(b) maximum allowable inelastic deformations,
(c) maximum stress/strain criteria under the complex multiaxial loading situation in the structure,

(3) Manufacturing and reliability: Existing manufacturing techniques involve Chemical Vapor Deposition (CVD), Chemical Vapor Infiltration (CVI) and Hot Isostatic Pressing (HIP) technologies for the matrix. A wide range of fibers and architecture are also possible. The structural performance, lifetime and reliability are all dependent on the manufacturing method of the composite. In addition, cost is an important factor, which will be also determined by the manufacturing technique.

2.12. Critical issue no. 12: Validation of radiation shielding requirements, design tools, and nuclear data

Radiation shielding must protect both personnel and sensitive reactor components. Components with the most stringent protection requirements include the final optics in a laser-driven fusion reactor. Other components with important radiation protection requirements include magnets in the heavy ion driver, instrumentation and control. Two important requirements must be imposed on the radiation shield in order to enhance attractive environmental and safety features of IFE reactors. First, the bulk shield (immediately surrounding the blanket) must be designed so that the long-term activation in reactor components outside the cavity and inside the reactor building is minimum. Such components include the heat transport system, heat exchanger and/or steam generators, and a variety of auxiliary systems and constitute a large material inventory that would tremendously increase the waste disposal problem if allowed to be highly radioactive. Second, the IFE shield should be designed to permit some personnel access to the reactor building outside the bulk shield within days after shutdown. Although full remote maintenance should be planned for, having personnel access capability after shutdown is deemed necessary in a number of foreseen cases and unforeseen events.

These critical requirements on the shield combined with the fact that the shield is one of the largest (in volume and weight) and more expensive components in an IFE reactor necessitate careful shield design. Sophisticated capabilities for predicting the radiation field and associated radiation response in materials are required. Although advanced capabilities exist, uncertainties in accuracy remain due to modelling complexities, nuclear data uncertainties, limitations of calculational methods in void regions and deep radiation penetration problems, and time dependent behavior of materials and components. For example, it is likely that components will deform during operation, which may lead to unpredictable streaming paths. Improvements in methods, data and experimental verification of prediction capabilities are needed.

Establishing accurate radiation protection requirements is necessary, particularly for components whose shielding is either physically difficult (e.g. final optics in laser driver) or results in substantial economic penalty. Thus, quantitative and reliable knowledge of

the effect of radiation on materials and components is required.

2.13. Critical issue no. 13: Reliability and lifetime of laser and heavy ion drivers

Description of the problem – The reliabilities and lifetimes of excimer laser and heavy ion driver systems profoundly affect the operating characteristics of an inertial fusion energy (IFE) reactor. Although both the excimer laser and the heavy ion are powered with somewhat similar pulsed power systems, the critical issues associated with these two drivers are sufficiently distinct that they should be considered separately. There are presently no known technical problems which could keep either of these driver types from performing reliably as IFE drivers.

Reliability and lifetimes of excimer laser drivers – Two general types of excimer laser amplifiers have been considered for IFE:

(1) Direct electron-beam pumping through a foil, and
(2) Electric-discharge pumping.

The first category can be constructed in larger sizes (and hence output energies) than the latter. Theoretical simulations suggest that the electric-discharge laser may be more reliable than the e-beam pumped laser. There are, in addition, a number of similarities which these two types of excimer lasers share. First of all, a key parameter for each of the lasers is the small signal optical gain, G_o given by the expression:

$$G_o = \exp(\sigma N L), \tag{23}$$

where σ is the stimulated emission cross-section for the excimer laser transition, N is the inversion density of the excimer laser amplifier, and L is the length of the active excimer gain medium. Typically, G_o must be less than some fixed number (such as 20–30) in order to avoid unwanted parasitic oscillations in the amplifier volume. A somewhat higher limit is set by the superfluorescent limit which defines a relationship between the amplifier solid angle, Ω_a, and the small signal gain, G_o. A simplified expression [13] for the superfluorescent limit on amplifier gain is given by the expression:

$$4\frac{\sqrt{\ln G_o^2}}{\sqrt{(G_o - 1)^3}} < \Omega_a, \tag{24}$$

where the amplifier solid angle is given approximately by d_a^2/L^2 for a rectangular amplifier (where d_a is the amplifier aperture). Since σ is nominally a fixed parameter, in order to keep G_o below the parasitic limit, L and/or N must be adjusted. The difficulty here is that the excimer inversion density, N, is related to the inversion energy, E_s, in the medium given by the expression:

$$E_s = Nh\nu L d_a^2, \tag{25}$$

where, as before, d_a is the amplifier aperture, h is Planck's constant, and ν is the laser frequency. An important parameter for laser amplifiers is the inversion energy per unit volume, $\rho_s = E_s/V = Nh\nu$. In optimizing amplifiers, frequently ρ_s is maximized in order to obtain the highest output energy/cm^3 form the excimer amplifier gain volume. A typical limit for ρ_s is 20 J/l, or more typically 10 J/l [13]. Thus, in order to keep G_o below either the parasitic limit or the superfluorescent limit, it is easiest to adjust L, the gain length. In carrying out these optimizations at constant σ and N, the results tend to reduce the size of the excimer laser amplifier to dimensions of the order of $50 \times 50 \times 200$ cm with a volume of approximately 500 liters. Amplifiers this size tend to produce less than 5 kJ of output energy, an amount of energy which is only 0.1% of the total driver energy of 5 MJ; this is an important factor in performing the overall Prometheus failure mode analyses. Designers of e-beam pumped lasers, however, have produced designs for much larger amplifiers, theoretically producing output energies of hundreds of kilojoules.

Each of these two types of excimer lasers is briefly described below:

E-beam pumped excimer lasers – Direct electron-beam pumping permits large volumetric excitation of the excimer gain media (typically a mixture of noble gasses plus a halogen). All of the pumping energy delivered to the gas is delivered by the e-beam. This excitation scheme has been attractive for the construction of large excimer lasers since it is readily scalable to large apertures (~ 100 cm), energies, and volumes (thousands of liters).

The e-beam is generated under hard vacuum conditions (10^{-7} torr or better), whereas the excimer gain medium has a density of approximately 1 amagat (corresponding to a gas pressure of 760 torr). A thin foil is used to separate the high vacuum e-beam from the corrosive halogen atmosphere inside the laser amplifier. Since the excitation area is given by the product $d_a L$, a relatively large foil area in a typical e-beam pumped excimer laser amplifier (such as the LAM [14] with a $\sim 100 \times 200 = 2 \times 10^4$ cm^2 area) is exposed to the vacuum interface. In order for the thin (several micron) foil mechanically to support the force exerted

by the 760 torr differential pressure, a mechanical bridge-type structure (often referred to as a Hibachi) which may block a portion of the incident e-beam is installed to stiffen the foil structure. In operation, the high power e-beam is accelerated through potentials in excess of 10^6 V, and upon traversing the foil, some fraction (30–50%) of the electron beam energy is lost. The action of this large amount of energy is deposited into the small volumes of the foil and Hibachi, thereby greatly stressing these elements, particularly the foil in cases in which the beam current density is not uniform. The problem increases significantly in repetitive operation since it necessitates water-cooled Hibachis. In some cases, the repetitive operation of an e-beam pumped excimer laser has hitherto been unreliable because of periodic foil ruptures. In order to overcome this problem, e-beam pumped excimer lasers have received a considerable amount of technological development.

Even with the greater energy capabilities of EBELs, a substantial number, n, of EBELs is required to generate the ~ 5 MJ of energy required for the Prometheus laser driver. (The required laser energy on target is 4 MJ but, owing to optical inefficiencies associated with beam combination, propagation, and pulse compression, the output energy from the EBELS needs to be at least 25% greater than the desired net energy). Assuming that each of the n optimized e-beam pumped excimer amplifier produces an output energy $= 5$ MJ$/n$ (which is presumably more than 1% of the total driver output energy), the mean number of amplifier firings between failures must be at least $n \times 10^8$ if the IFE reactor operation is not to be interrupted between annual maintenance periods.

Electric-discharge excimer lasers – Much less experimental work has been carried out on electric discharge excimer lasers. In this case, excitation of the excimer gain medium occurs on the neutral channel with relatively low-lying energetic species being produced. This can enhance the efficiency of the laser amplifiers. Unlike the e-beam pumped excimer laser, the full pumping power does not flow through a foil/Hibachi structure, and predictions are that this design could be made more reliable following an intensive development effort.

Owing to the nature of the electric discharge, the available pulse duration is shorter than that for the e-beam (200 ns compared with ~ 500 ns). Electric discharge lasers for which $d_a > 30$ cm appear to have serious discharge stability and efficiency problems. As a consequence, using the scaling relations outlined above, the electric discharge lasers tend to optimize at energies of a few kilojoules. For energies this small, the overall reliability of the IFE reactor would not be impaired if several electric discharge amplifiers failed. Assuming such amplifiers could readily be replaced by robotics, the impact of discharge amplifier failure on reactor operation is regarded as minimal. As a consequence, if failed electric discharge excimer lasers can be replaced more rapidly than they fail, then the mean time between failure characteristics of the IFE reactor will be independent of the excimer amplifiers.

Reliability and lifetimes of heavy ion drivers – The fundament of an efficient, reliable Prometheus heavy ion driver is the successful design, construction, and testing of a full scale accelerator suitable for operation in a burst mode (~ 50 kHz) to fill storage rings with 18 beamlets at a rate of ~ 360 pulses/s. Accelerators can be made to be very reliable if great care is taken with regard to the control of the magnets, particularly in the (recommended) case of superconducting dipoles, quadrupoles, and triplets. A large amount of data is available on the failure modes of linear accelerators (LINACs), and there are no serious technical problems which would render this design unreliable. The key element for long, reliable operation of the LINAC is a very fast, highly automated control system which can sense beam mispointing before superconducting magnets are either heated sufficiently to make them go "normal" or be damaged by the beam. Under competent computer control, the heavy ion driver would only require attention during regular IFE reactor maintenance intervals (possibly every two years). A key element in this HI driver reliability assessment is the development of an adequate computer control system employing the latest developments in artificial intelligence, parallel processing, and expert systems (see ref. [1], Section 6.5.3.3).

Accurate simulations of the dynamics of the LINAC, the filling of the storage rings, the bunching, the rapid expansion to the triplet focusing magnets, the focusing down into the pre-formed channels, the complete stripping of the heavy ions, and the dynamics of self-focused heavy ion beams propagating down the channels to the target are too difficult to attempt presently, and the results, even if favorable, would require experimental verification to be trusted. Thus, the major emphasis on demonstrating the feasibility of heavy ion drivers should be experimental.

It is essential that a carefully planned heavy ion driver developmental program be designed to test each of the key elements of the proposed Prometheus-H IFE heavy ion driver in order to create a design data base sufficient to permit suitable modifications allow-

ing the driver to reach its full reliability potential. In particular, experimental results on beamlet accumulation (without emittance growth) for ms time scales in storage rings, self-focused beam stabilities, locking the focused beams into a pre-formed channel, etc., are crucial for developing this promising driver concept.

2.14. Critical issue no. 14: Demonstration of large-scale non-linear optical laser driver architecture

Description of the problem – The fundament of the Non-Linear Optical Subsystems proposed for the Prometheus-L driver is based upon the very strong experimental and theoretical bases of non-linear optics. Since both proposed subsystems are simply large optical cells filled with H_2 and SF_6 respectively, there are very few components present which can fail. The primary question is how well the system will function properly on the first pulse. If the electro-optical subsystems can be tailored to achieve first time operation, the overall architecture should prove to be as reliable as other state-of-the art, high speed, high voltage electronics. A balance must be struck between the extremely high gains (and concomitant high conversion efficiencies) of which these systems are capable. Thus, the reliabilities and lifetimes of the two types of non-linear optical subsystems proposed for the Prometheus-L IFE reactor design hinge primarily on the support optical equipment that is associated with the non-linear optical (NLO) devices. The two NLO devices are:

(1) the Raman accumulators, and
(2) the SBS pulse compressors.

Numerous key non-linear optical (NLO) subscale experiments and analyses have been performed in the last twenty years which demonstrate the capabilities of these two types of NLO devices. In order to properly implement them, however, each needs to be supplied a Stokes seed beam, and therein lies most of the questions regarding the success of the architecture reliabilities and lifetimes.

Generation of Stokes seeds for Raman accumulators – To achieve highest efficiency while averaging excimer laser intensities across the accumulator aperture, the proposed Prometheus Raman accumulator system uses crossed stimulated rotational Raman scattering. This architecture sets limits on the bandwidth, $\Delta\nu_{\text{lasers}}$ of the excimer pumps, on the crossed Raman angle, θ, and on the dimensions of the gain length (to avoid generating higher order Stokes beams). The physics is relatively well understood. A detailed design could be made now using present understanding. Tests at full scale could be made if approximately 30 two-kilojoule KrF excimer laser amplifiers were available as pump sources.

The required Stokes seeds can be derived from taking a small portion of the available excimer pump light, injecting the pump light into a Raman oscillator filled with the same gas used in the Raman amplifier. This process generates an automatic frequency shift, $\Delta\nu_R$, equal to the required Raman shift. Injecting this Stokes seed beam into the Raman amplifier at an angle θ to the pump beams permits a high quality (in the case of the Prometheus-L design, 80 kJ) output beam to be generated following path matching of the seeds to the original pump beams.

If stimulated rotational Raman scattering proved to be too difficult to control under the required test conditions (higher order Stokes, etc.), stimulated vibrational Raman scattering could suffice, at a slight reduction in overall operating efficiency. The Raman accumulators should be able to achieve high degrees of reliability.

Generation of Stokes seeds for SBS pulse compressors – The Stokes seeds for the SBS pulse compressors are generated electronically by "chirping" (acoustical-frequency shifting) the leading edges of the 80 kJ output beams from the Raman accumulators. Some technological development needs to take place to permit full aperture "chirpers" to be installed, but subscale tests with small crystals have produced promising results. Work at the Lawrence Livermore National Laboratory has already produced Pockels cells having conducting electrodes with apertures of approximately 30 cm. Experimental verifications need to be made of theoretical predictions of compressed pulse shapes and conversion efficiencies given the specific requirements on pulse shape established by the Target Working Group.

In the same vein, fast, large aperture ($\sim$ 100 cm) Pockels cells to be used for pulse-shaping the depleted pump beams from the SBS pulse compressors for synthesizing the required precursor pulses need to be demonstrated.

Although the development of large aperture Pockels cells may prove difficult, there do not appear to be any serious technological problems associated with synthesizing large aperture electro-optical (E/O) switches from smaller components. This synthesis may have significant advantages, for example, in the suppression of transverse SBS losses in the Pockels cells.

The SBS pulse compressors and attendant E/O switchyards currently represent the highest risk elements in the Prometheus-L driver design. Failure of

any of the Pockels cells or "chirper" modulators would mean the loss of an entire 80 kJ beamline, with consequent failure of direct drive targets. In some cases, continued operation with indirect drive targets could be considered even if one of the 80 kJ beamlines went down.

2.15. Critical issue no. 15: Demonstration of cost effective KrF amplifiers

One of the key elements associated with developing a cost effective KrF laser driver for the Prometheus reactor design study is the design of the output KrF laser amplifier module. These KrF amplifier modules represent the fundamental building-blocks of the KrF driver, generate the output energy pulses for the KrF laser driver, and the nature of their design represents a major foundation of the laser driver reliability. These KrF amplifiers need not only meet requirements of output energy, pulse duration, beam quality, beam diameter, wavelength, bandwidth, etc., but also stringent requirements on reliability, consistency of operation, etc. In order to prevent catastrophic failure of the IFE reactor, the Prometheus-L design has proposed a laser driver which can permit the occasional failure of a single KrF amplifier without requiring the concomitant shutdown of the reactor. As this freedom from KrF amplifier failure is predicated upon the choice of IFE reactor operation with direct drive targets, a limit is placed upon the laser energy delivered by each KrF amplifier such that the 1% direct drive target illumination uniformity requirement is met. Given 60 beams arranged symmetrically around the spherical direct drive target, together with a nominal laser driver energy of 5 MJ, the loss of 5 kJ (or approximately 6%) from each of the 60 beams from time to time should still permit target illumination uniformity to be maintained, at least for tangential target illumination schemes. KrF amplifier output energies of 5 kJ represent a significant derating of current designs and successful development of reliable amplifier prototypes should be achievable during the next decade if sufficient funding is made available.

Previous Department of Energy (DOE) and Department of Defence (DOD) excimer laser research and development programs have identified two general excimer laser amplifier design configurations:

(1) Direct electron beam excitation of relatively large ($V > 1000$ liters) excimer laser amplifier volumes, and
(2) Electric discharge excimer laser amplifiers with the excitation of the KrF excimer achieved along the neutral channel for geometries involving moderate ($V < 200$ liters) volumes.

The first excimer laser amplifier design configuration, electron beam excited excimer lasers (EBEL), has received extensive development from both the DOE and the DOD with KrF amplifier modules as large as 2000 liters being constructed. The second configuration, electric discharge excimer lasers (EDEL), has been much less thoroughly investigated; some preliminary theoretical work was funded by DOE [15] several years ago, but little experimental verification of the predicted high EDEL efficiency was made. Each of these two KrF amplifier design configurations has its supporters and detractors. The EBEL has received priority development over the EDEL because the EBEL scales to larger volumes (and hence larger output energies) much more readily than does the EDEL. For single-shot DOE applications and for some DOD applications, this scalability advantage of the EBEL has been important. For an IFE reactor application in which reliability for a 10^9 shot over long periods of time at repetition rates of 3–10 Hz is crucial, the potentially higher reliability of the EDEL makes this configuration of greater interest than formerly.

During the course of the reactor design study (including reviews with Government scientists), the question has been raised whether or not KrF amplifiers can be designed to fulfill all the technical requirements (summarized below), while still achieving a cost effective level of performance to permit the overall cost of electricity (COE) for the IFE reactor to be competitive. Our design should significantly reduce the risk of developing a cost-effective KrF final amplifier design for three reasons:

(1) The amplifier output energy has been reduced from the 250 kJ level suggested for EBELs down to levels of the order of 5 kJ,
(2) Since the dimensions of the Prometheus-L excimer laser amplifier are of the order of $30 \times 30 \times 200$ cm, parasitic oscillations and superfluorescent losses are more easily controlled,
(3) Optics costs and risks are significantly reduced as the effective aperture of the amplifier is reduced to 30 cm.

The new non-linear optical beam combination design approach which has made it technically feasible to relax the energy, volume, and aperture requirements for the KrF laser amplifiers is the implementation of forward stimulated rotational Raman scattering amplifiers for beam combination, larger aperture synthesis, and improved beam quality. Nonetheless, there remain

Table 5
Design requirements for EBEL

Requirement description	Design value
Output energy	240 kJ
Amplifier aperture	3×3 m
Pulse duration	500 ns
Amplifier volume	54 m^3
Amplifier gain length	6 m
Amplifier gain coefficient	0.023/cm
Energy storage density	7 J/liter
Energy extraction efficiency	0.7
Final anode voltage	3.3 MV
Overall efficiency	10%
Bandwidth	1% or 10^{13}Hz
Laser wavelength	248 nm
Active medium	KrF
Total gas pressure	760 torr
Pulse compressor	angular multiplexing
Laser beam quality	1.4 XDL
Peak to peak laser beam homogeneity	20%
Number of shots between failures	10^{10}
Repetition rate	5 Hz

Table 6
Design requirements for EDEL

Requirement description	Design value
Output energy	4 kJ
Amplifier aperture	30×30 m
Pulse duration	200 ns
Amplifier volume	0.18 m^3
Amplifier gain length	2 m
Amplifier gain coefficient	0.05/cm
Energy storage density	22 J/liter
Energy extraction efficiency	0.7
Final anode voltage	50 MV
Overall efficiency	12%
Bandwidth	10^{10}Hz
Laser wavelength	248 nm
Active medium	KrF
Total gas pressure	760 torr
Pulse compressor	chirped SBS
Laser beam quality	1.1 XDL
Peak to peak laser beam homogeneity	5%
Number of shots between failures	10^9
Repetition rate	5 Hz

a series of developmental problems associated with both types of amplifiers.

In evaluating the relative risks associated with the two excimer laser designs, the requirement performance parameters of each is summarized below in Table 5 and Table 6. Note that the large volume EBEL

Table 7
EBEL developmental problems

#	Description of problem area	Possible solution
1	Foil rupture	Homogenize E-beam current density
2	Parasitic oscillations	Lower amplifier reflectivities
3	Amplified superfluorescence	Reduce amplifier solid angle
4	High cost of large windows	Segmented optics
5	Radiation damage from E-beams	Lower anode voltage
6	Reduced beam quality	Phase conjugation
7	Optics damage	Reduce radiation fluence
8	Catastrophic failure mode	Redesign foil support structure

Table 8
EDEL developmental problems

#	Description of problem area	Possible solution
1	Stabilization of discharge	Discharge uniformity; control F_2 burn
2	Uniformity of discharge excitation	Elimination of cathode fall region
3	Reduced excimer beam quality	Beam combination in Raman cell
4	Achieve 10^9 shot lifetime	Engineer pulsed power/electrodes
5	Optics damage	Reduce radiation fluence
6	Verify excitation efficiency	Conduct full scale experiments

amplifier module must have a saturating laser pulse passing through the active volume in order to prevent serious superfluorescence and parasitic oscillation losses associated with the high (13.8 neper) small signal gain of the amplifier.

Comparison between Table 5 and Table 6 will indicate that the requirements for the EBEL are generally much more difficult to attain than those listed for the EDEL, with regard to the required optics, the pulsed power, and the performance of the amplifiers themselves. The key developmental problems associated with each of these two types of excimer laser amplifiers are summarized below in Tables 7 and 8.

These EBEL developmental problems are relatively well understood in view of the extensive theoretical and experimental studies of these amplifiers carried out by both the DOE and the DOD. For successful implementation into an IFE reactor, the most important development for the EBEL is the need for a dramatic increase in the mean number of amplifier firings between failures. As summarized in Table 7, there are also significant problems associated with the EDEL approach, but since the amount of research and development for these amplifiers is relatively small, larger uncertainties in this excimer laser design exist. Compared with the EBEL, the developmental problems for the EDEL appear to be more tractable although relatively little work to date has been completed for these devices.

Summary

Considerable developmental work has been carried out during the last decade on EBEL amplifiers. Although much progress has been made in achieving the ambitious design goals for EBEL amplifiers, these devices are currently not believed to be capable of meeting a 10^9 shots-between-failure requirement. Moreover, the primary advantage of the EBEL design over the EDEL is the ability of the e-beam excitation to scale to larger amplifier volumes. This is not desirable for a reactor design since it causes the excimer laser amplifier to become the cause of a single point failure.

It must be emphasized that significant KrF amplifier development work must be carried out in the next decade if the demanding requirements for the KrF driver amplifiers are to be met. Thus, the essence of this Critical Issue is that substantial development effort will be required in order to provide the KrF amplifiers which will be the workhorses of the future IFE reactor. Details are defined in the associated Research and Development section.

2.16. Critical issue no. 16: Demonstration of low cost, high volume target production techniques

Description – Target production for IFE reactors will require technologies which are presently either nonexistent or insufficiently developed for such an application. It is, therefore, very difficult to accurately estimate the production costs of such targets. These difficulties are further aggravated by the potential need for sabots to deliver the targets to the reaction chamber and, in the case of indirect drive, for an outer case which must meet stringent engineering requirements. Target cost is clearly a critical issue in light of the fact that IFE reactors will consume huge numbers of targets (on the order of 10^8 per year), and will be uneconomical and, therefore, impractical if these targets are too expensive.

3. Comparison of IFE designs

3.1. Introduction

There are several design and technology options for inertial confinement fusion reactors, e.g. laser and heavy ion drivers, direct and indirect drive targets, and dry and wetted first walls. Comparison among options is normally sought by scientists and programmatic decision-makers in order to select, or at least reduce, the number of options that are worthy of further research and development (R&D).

A quantitative methodology is needed as a tool in comparing and selecting among options. However, in some important cases, the basic information required to perform this quantitative comparison is lacking. This tends to discourage the technical community from pursuing any quantitative comparison. Since decisions to narrow design and technology options for further R&D must be made one way or the other in a budget-constrained program, the lack of a clear comparative methodology means that decisions would have to be made based on "expert judgment". Quite often the experts disagree on their preferred choices and the reasons for disagreement may not be known. In the Prometheus study, a clear comparative methodology was developed. In applying this methodology, some data were not available and a "best guess" by technical experts was used for such data. The results of the comparative evaluation were analyzed and discussed by experts who attempted to formulate conclusions. One key advantage of using a quantitative, comparative methodology is that, if differences among experts arise

regarding a particular piece of data or interpretation of the comparative analysis results, the reasons for the differences and methods for resolving them become clear. One other key advantage is that through the "process" of applying a quantitative methodology, experts gain much better insight into important areas of differences among design and technology options. Such insight makes experts better able to make more informed decisions even if the results of the comparative analysis do not show a clear-cut conclusion.

Section 3.2 presents the highlights of the Evaluation Methodology developed in the Prometheus study. The methodology has utilized previous work when available, e.g. refs. [16], [17] and [18]. Section 3.3 summarizes the results of applying this methodology to compare the Laser-Driven and Heavy-Ion Driven reactor designs of Prometheus. Although the methodology is discussed and applied here for comparing the two IFE designs, the methodology framework is general enough to allow extension in the future for comparing other options, e.g. comparing inertial and magnetic fusion reactors.

3.2. Evaluation methodology

Design options for power plants that can be constructed today can generally be compared based on economics and safety and environmental attractiveness. However, fusion is in a relatively early stage of research and development. The data base is incomplete and success in developing particular design options for subsystems cannot be assured. Designers have to extrapolate present knowledge to predict performance in fusion power reactors, with the degree of extrapolation varying greatly from one design option to another. Furthermore, there are substantial differences among proposed design options in the probability of success and in the time and cost required to develop these options. Therefore, a prudent evaluation methodology for comparing fusion reactor conceptual designs must account for these differences.

Five major areas of evaluation are established. These are:

1. Physics Feasibility
2. Engineering Feasibility
3. Economics
4. Safety and Environment
5. Research and Development Requirements

Each of the above areas is quantified through a system to be described shortly. In this system, a number of detailed criteria are developed for each area. For each criterion, there is an attribute (index) that can be quantified. A weighting scale is devised for the attributes. The weighted sum of the attributes for each evaluation area represents a score for this area.

The result of the evaluation process for a given reactor design concept is a numerical score for each of the five evaluation areas. No mixing of the scores for

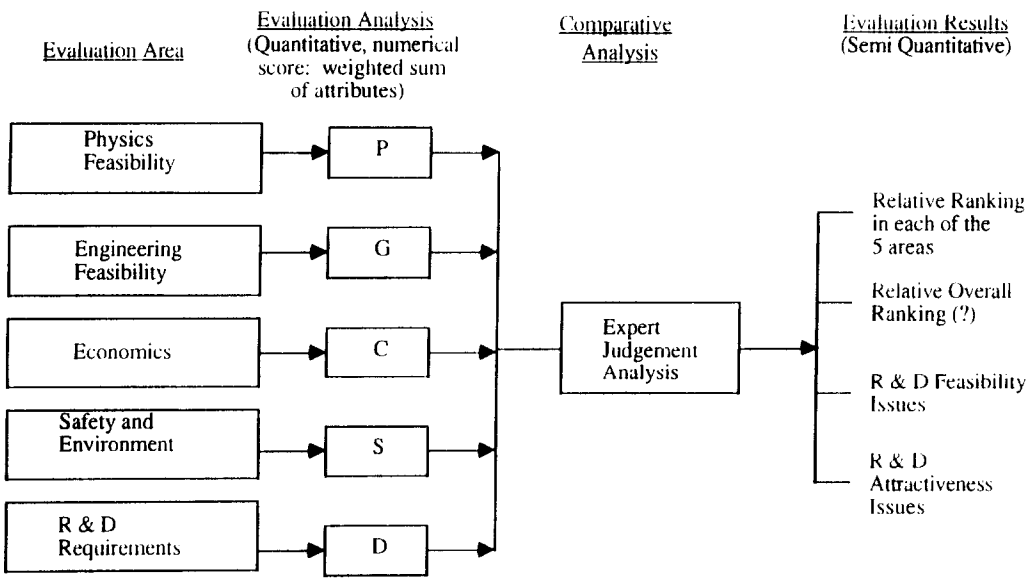

Fig. 22. Evaluation methodology approach.

the five evaluation areas is allowed, i.e. the numerical scores for the five areas are not combined to derive one final composite score. Instead, the comparison among reactor design concepts will involve comparative analysis of the scores for the five areas. A panel of knowledgeable experts can interpret the results given in the scores in each of the five evaluation areas. The evaluation approach is highlighted in Fig. 22.

The results of such evaluation will undoubtedly be impacted by the many choices that designers select. For this study, it is very important for the comparative evaluation to distinguish between the effects on the scoring results of generic and non-generic choices for the design. For example, the tritium breeding blanket is necessary for all fusion reactors. However, selection of low activation structural material is not a necessity, but a designer's choice. Therefore, comparing a reactor concept with low activation materials to another reactor design with high activation structural materials (or vice versa) cannot be permitted unless it is shown that these selections are dictated by inherently different requirements in the designs being compared.

Below is a description of the evaluation system for each of the five evaluation areas.

Physics feasibility – Physics feasibility is clearly a requirement for acceptance of any reactor design concept. However, the required and achievable physics performance goals vary from one reactor concept to another; for example, the fusion yield in directly and indirectly-driven targets in laser and heavy ion reactors and β (ratio of plasma-kinectic to magnetic pressure) in magnetic fusion reactors. In IFE reactors, physics feasibility extends beyond the physics of implosion to cover other physics areas associated with the driver and driver-target coupling.

This work did not attempt to develop a general methodology for comparative evaluation of physics feasibility for all options. Rather, a specific methodology was developed to compare the physics feasibility in laser and heavy ion-driven reactors. This methodology is presented in Section 3.3.2 together with the application to compare Prometheus-L and H.

Engineering feasibility – Present conceptual designs are based on extrapolations from present engineering knowledge and experience. Hence, there are uncertainties in the ability of present conceptual designs to meet their goals. These uncertainties vary from one design to another depending on the degree of extrapolation and optimism that lead to better performance, which is rewarded indirectly in the "economics" and "safety and environment" categories of the evaluation criteria. One key purpose of the "engineering feasibility" cate-

Table 9
Engineering feasibility evaluation

	Weight
Ability to meet design goals	(0.60)×
1. Component fabricability	0.1
1.1 First wall	×0.35
1.2 Blanket	×0.20
1.3 Driver	×0.15
1.4 Beam transport	×0.15
1.5 Final optics	×0.15
2. Subsystem performance goals	0.3
2.1 Cavity	×0.4
2.1.1 First wall protection	×0.5
2.1.2 Blanket	×0.5
2.2 Fusion reaction support systems	×0.6
2.2.1 Driver	×0.2
2.2.2 Beam transport	×0.2
2.2.3 Final optics	×0.2
2.2.4 Target fabrication	×0.2
2.2.5 Target injection	×0.2
3. Tritium fuel self-sufficiency	0.2
4. Reliability goals	0.1
first wall	×0.35
blanket	×0.20
driver	×0.15
beam transport	×0.15
final optics	×0.15
5. Maintainability	0.1
first wall	×0.35
blanket	×0.20
driver	×0.15
beam transport	×0.15
final optics	×0.15
6. Lifetime goals	0.1
first wall	×0.35
blanket	×0.20
driver	×0.15
beam transport	×0.15
final optics	×0.15
7. Cost projections	0.1
cavity	×0.25
driver	×0.25
target manufacture	×0.25
BOP	×0.25
Ultimate potential	(0.4)×
8. Potential for inherent safety	0.25
9. Potential for low long-term activation	0.25
10. Engineering simplicity	0.3
individual system complexity	×0.5
interdependence of systems/functions	×0.5
11. Operating requirements	0.10
12. Potential for enhanced energy conversion efficiency	0.10

Table 10
Scoring system for engineering feasibility

	Score
Component fabricability	
existing technology	3
direct extrapolation of existing technology	2
new technology	1
Subsystem performance goals	
demonstrated performance in existing facilities	3
uncertain, but judged to be resolvable with R&D	2
highly uncertain – may be impossible	1
Ability to achieve tritium fuel self-sufficiency (margin = $\lambda_a - \lambda_r$)	
$\lambda_a - \lambda_r > 0.2$	3
$\lambda_a - \lambda_r > 0.1$	2
$\lambda_a - \lambda_r < 0.1$	1
$\lambda_a - \lambda_r < 0.0$	0
Reliability goals	
goals based on extrapolation of relevant data	3
little data, but confidence in estimates	2
little confidence in estimates	1
Maintainability	
maintenance achieved by demonstrated methods	3
some novel or complex maintenance procedures	2
system availability depending on novel or complex procedures	1
Lifetime goals	
credible data exists to support lifetime estimate	3
existing data can be extrapolated to support goal	2
little or no data to support lifetime estimate	1
Cost projections	
credible data exists to support cost estimate	3
existing data can be extrapolated to support estimate	2
little or no data to support cost estimate	1
Potential for inherent safety (IS)	
no reason inherent safety couldn't be achieved	3
some sources/pathways may prevent IS	2
some features of design probably prevents IS	1
Potential for low long-term activation (LTA)	
no sources of LTA	3
sources of LTA could be eliminated with R&D	2
sources of LTA inherent to design	1
Engineering simplicity	
simple design and/or operation	3
some complex aspects of design and/or operation	2
highly complex aspects of design and/or operation	1
Operating (e.g., startup-shutdown) requirements	
response times < hours	3
response times > hours	2
off-normal operation puts plant or personnel at risk	1
Potential for enhanced energy conversion efficiency	
well-defined options exist	3
some speculative options exist	2
no credible means known to significantly improve efficiency	1

gory is to scrutinize, assess and calibrate such extrapolations and provide a figure of merit to balance "questionable rewards" made in other categories of the comparative evaluation. Another key purpose of engineering feasibility is to evaluate areas where certain goals must be met, e.g. tritium self-sufficiency, in order for the reactor design concept to be acceptable.

The engineering feasibility category is divided into two subcategories:
(1) Ability to achieve design goals
(2) Ultimate potential.

The first subcategory provides a measure to account for uncertainties in achieving the design goals. The second provides a measure for comparing the practicality of various designs in ultimately reaching very desirable goals such as inherent safety, low long term activation; and enhanced energy conversion efficiency.

The figure of merit for Engineering Feasibility, G, is obtained as follows:

$$G = W_a I_a + W_p I_p, \tag{26}$$

where
W_a = weighting factor for the "ability to meet design goals" subcategory,
I_a = score for "ability to meet design goals" subcategory,
W_p = weighting factor for the "ultimate potential" subcategory,
I_p = score for the "ultimate potential" subcategory.

W_a is assigned 60% while W_p is assigned 40% to reflect the notion that the ability to meet design goals has somewhat higher priority than capabilities to ultimately reach desirable goals.

Each subcategory is further divided into a number of attributes (indices), each has a weight and score. The score for each subcategory is obtained as the weighted sum of the scores for the attributes.

Table 9 shows the various indices and assigned weights. A scoring system has been devised so that the maximum score for any given index is 3. Since the sum of the weights for all indices is 1.0, the maximum score

for "Engineering Feasibility", G, is 3. Table 10 shows the scoring system for engineering feasibility.

Economics – A single figure of merit, cost of electricity, is adopted. Use of the cost of electricity as a figure of merit integrates the weighted effects of capital and operating costs, replacement time and frequency, fusion power, thermal power conversion efficiency and recirculating power requirements.

The "first year" cost of electricity in then-year dollars is defined by the following equation:

$$\mathrm{COE} = \frac{(\text{Annualized Capital Cost}) + (\text{Yearly Operating Cost})}{(\text{Net Power}) \times (\text{Plant Availability}) \times (\text{Time})},$$

$$\mathrm{COE} = \frac{(\mathrm{DC} + \mathrm{SPR} + \mathrm{CTGY} + \mathrm{ID} + \mathrm{INT} + \mathrm{ESCL})\mathrm{FCR} + (\mathrm{O\&M} + \mathrm{SCR} + \mathrm{FUEL})(1 + \text{ESC Rate})^{\mathrm{YRS}}}{(\text{Thermal Power} \times \text{Gross Effcny} - \text{Recirc Powr}) \; (\text{Availability})[\mathrm{hrs/y}]},$$

where

COE = cost of electricity,
C = figure-of-merit for the economics evaluation area,
DC = direct capital costs,
SPR = spare parts allowance (2 to 4%),
CTGY = contingency allowance (15% of direct costs),
ID = indirect costs,
INT = interest during construction (based on 10% cost of money over construction period),
ESCL = escalation during construction (based on 5% escalation over construction period),
FCR = fixed charge rate (nominally 15%),
O&M = operations and maintenance cost,
SCR = scheduled component replacement cost,
FUEL = annual fuel cost,
ESC RATE = annual escalation rate (5% per year),
YRS = construction period.

The cost of electricity is the total busbar energy for the first year of operation. The total capital investment is equally divided and charged to the annual operating periods through the use of a fixed charge rate. Annual operating costs are also included with appropriate escalation from the year of the estimate (start of construction) to the initial operation date (see ref. [1], fig. 3.5-1 for specific economic guidelines and bases used in this study).

Safety and environment – One of the most important incentives for fusion energy development is its potential safety and environmental attractiveness. Therefore, enhancing safety and environment features in fusion reactor designs is important for the ultimate acceptance of fusion. The purpose of the Safety and Environment evaluation area is to measure the relative safety and environmental attractiveness of various design concepts.

Limitations on study resources and deficiencies in present knowledge preclude performing a complete probabilistic risk assessment to obtain a single figure-of-merit for the total risk to the public. Therefore, a simpler approach is adopted based on a method developed earlier in BCSS [18]. Three subcategories are defined for the Safety and Environmental area, as shown in Fig. 23 and listed below.

(1) Source Term Characterization (I_1),
(2) Response to Accidents (Fault Tolerance) (I_2),
(3) Non-Accident Concerns (I_3).

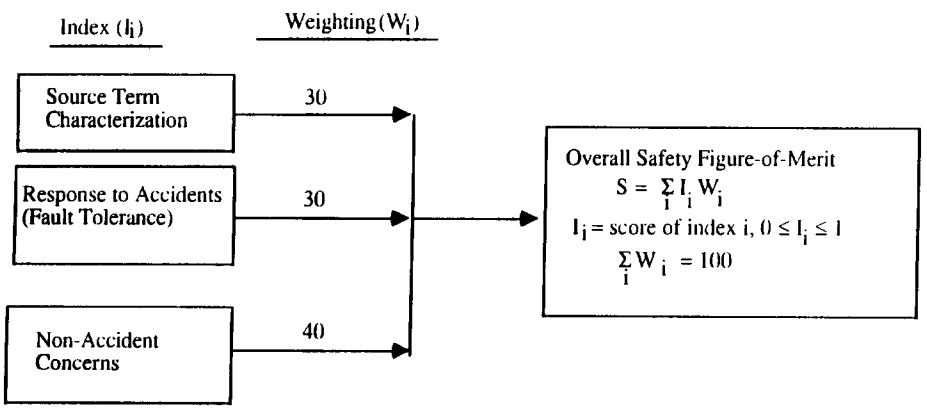

Fig. 23. Safety and environment evaluation approach.

The attribute for each subcategory, I_i, is measured on a scale from 0.0 to 1.0 and has a weighting value, W_i. The overall figure of merit (S) for the safety and environmental area for a given reactor design concept is defined as

$$S = \sum_{i=1}^{3} I_i W_i, \tag{27}$$

with

$$\sum_i W_i = 100. \tag{28}$$

The weights given to each of the three subcategories are shown in Fig. 23.

Subcategory 1 is a measure of the component of accident risk from the radioactive and chemical source term common to accident initiators. The value of the attribute, I, for this subcategory is obtained from the scores of subindices, f_j, for key components of the reactor as:

$$I = \sum_j f_j \omega_j, \tag{29}$$

where $0.0 < f_j < 1.0$ and

$$\sum_j \omega_j = 1.0. \tag{30}$$

The weights assigned to various reactor components are given in Table 11.

The second subcategory relates to the likelihood and response to accidents. Again, the value of the attribute is obtained as the weighted sum of several indices related to the initiators of specific accidents. The indices, f_j, and weights, ω_j, for this subcategory are shown in Table 11. The third subcategory, non-accident concerns, has indices related to occupational

Table 11
Safety and environmental evaluation indices and weights

	ω_j
Source term characterization (score = I_S, W_S = 30%)	
Source term in target factory	0.2
Source term in the first protection chamberwall	0.2
Source term in the breeding blanket and shield	0.2
Source term in the driver	0.2
Non-radiological sources (e.g. fluorine)	0.2
Sum of weighted score for source term $I_S = \Sigma f_j \omega_j$	—
Response to accidents (fault tolerance) (score = I_R, W_R = 30%)	
Response to LOCA and LOFA in the first protection chamberwall	0.12
Response to LOCA and LOFA in the breeding blanket and shield	0.12
Response to beam pellet misfire accident in the chamberwall	0.12
Response to loss of coolant in the final optics or focusing magnet vacuum pumping system	0.12
Response to LOCA in the driver system	0.12
Fault tolerance to loss of T_2 and D_2 containers	0.10
Fault tolerance to containment integrity	0.10
Fault tolerance to target factory integrity	0.10
Fault tolerance to driver system	0.10
Sum of weighted score for response to accidents (score = $I_R = \Sigma \omega_j f_j$)	—
Non-accident concern (score = I_N, W_N = 40%)	
Occupational exposure (regular, maintenance)	0.25
Routine radioactive emission rate	0.25
Waste disposal (radiologial, hazardous, mixed)	0.20
Non-radiological hazards (florine, lead)	0.15
Heat dissipation	0.10
Construction impacts	0.05
Sum of weighted score for non-accident concerns $I_N = \Sigma f_j \omega_j$	—
Overall safety figure of merit = $W_S I_S + W_R I_R + W_N I_N$	—

exposure, radioactive emission rate waste disposal, non-radiological hazards, heat dissipation and construction impact. Each has an assigned weight as shown in Table 11.

Research and development requirements – One important figure of merit in comparing options for a future technology is the R&D required to realize these options. Since developing a complete R&D plan is not within the scope of this effort, the R&D required to provide the data base for design and construction of an experimental power reactor was evaluated for Prometheus type reactors as discussed in ref. [1].

The figure of merit for the R&D category of the Evaluation Methodology accounts for three important areas:

(1) Cost:
   (a) average annual operating cost,
   (b) capital cost of required facilities (new or upgrades).
(2) Time: total time to complete the R&D.
(3) Risk.

Measure of relative risk in not successfully resolving key issues weighted by the potential consequences of negative results.

The overall figure of merit (D) for R&D is written as

$$D = W_c R_c + W_t R_t + W_r R_r, \tag{31}$$

where R_c, R_t and R_r are the scores for cost, time and risk, respectively and W_c, W_t and W_r are the corresponding weighting factors.

Cost (R_c)

$$R_c = 0.5(A + F), \tag{32}$$

A = score for average annual operating cost,
F = score for capital cost of required facilities.

Average annual perating cost	Score A	Capital cost of required facilities *	Score F
> \$100 M	1	> \$500 M	1
\$50–100 M	2	\$200–500 M	2
< \$50 M	3	< \$200 M	3

* Summation for all key issues
* Specific dollar numbers for categories may change depending on the issues included and the purpose of comparison

Time (R_t)

R_t is the longest time required to resolve the issues. It is either cumulative time for sequential tasks or the longest time for parallel tasks. The score is according to the following table.

Time scale	Score R_t
> 30 yr	1
15–30 yr	2
< 15 yr	3

Risk (R_r)

The figure of merit, R_r, accounts for the probability of not resolving the key issues and the consequence of negative results. It is written as:

$$R_r = \frac{1}{3n} \sum_{i=1}^{n} P_i C_i, \tag{33}$$

where n = number of key issues. Dividing by the factor $3n$ ensures the maximum score for R_r is 3. P_i is the probability of not resolving the issue (negative result) and is assigned as follows:

Relative probability	P_i
Unlikely	3
Even (50/50)	2
Likely	1

C_i is the consequence of not resolving the issue (i.e. of negative results)

Relative consequence	C_i
Severe impact	1
Moderate impact	2
Low impact	3

3.3. Comparative evaluation results

3.3.1. Introduction

The evaluation methodology developed in the previous section was applied to compare the two inertial fusion reactor designs developed in this study: Prometheus-L, which is laser driven, and Prometheus-H, which is heavy-ion driven. The comparisons covered the five evaluation areas: physics feasibility, engineering feasibility, economics, safety, and environment R&D requirements.

The comparative evaluation effort attempted to rely on the quantitative data available from the conceptual

design study and other sources. However, limitations on time and resources available to this effort precluded complete quantitative analysis. Whenever data was not readily available, "expert judgment" was used. The following subsections present the results of the comparative evaluation in each of the five evaluation categories. A final subsection discusses the overall results.

3.3.2. Physics feasibilities of KrF and heavy ion inertial fusion energy

The physics feasibilities of both the KrF and the Heavy Ion drivers are described briefly below.

3.3.2.1. KrF laser IFE physics feasibility There are two parts to the physics feasibility of the KrF laser driver:

(1) The physics feasibility of the efficient interaction of the laser light with the direct drive DT target and its subsequent implosion (which may be beset with a variety of laser–plasma interactions driving Rayleigh Taylor Instabilities) or the physics feasibility of the efficient conversion of laser light into soft x-rays and the subsequent desired implosion of the DT fuel capsule in an indirect-drive target, and
(2) the physics feasibility of generating the specified DT target illumination conditions with regard to photon energies, phase distributions, intensity fluctuations, pulse duration, etc.

Although much can be written about the first category having to do with target interactions, and design, our primary responsibility during the Prometheus study has been to concentrate instead upon the second category, the physics feasibility of delivering appropriate laser pulses to either a direct-drive or indirect-drive DT fusion target. Included in the second category are the details of fabricating and delivering the DT target to an appropriate location for laser illumination and subsequent implosion.

The Prometheus KrF laser drive design is an extremely complex system composed of hundreds of thousands of elements, each of which will be required to perform at specified operating levels for a known length of time. The engineering feasibility of the laser driver defines the degree to which physically feasible elements have been designed and engineered in such a manner as to attain performance levels at or below limits defined by the fundamental physics of the element. In order to assess the physics feasibility of the laser driver design, it is necessary to analyze the fundamental operating principles behind the crucial elements of the laser driver. The criteria for establishing the Prometheus KrF Laser IFE driver physics feasibility are based upon answering the following questions:

(1) Does the intended operational mode of the device violate fundamental physics relationships?
(2) Can a self-consistent theory be developed which is capable of simulating the operation of the device in the ranges of interest?
(3) If a self-consistent theory is developed, are there highly unstable regions in operational phase-space which could produce significant fluctuations or undesired interactions with other systems?
(4) If the device is to be integrated into a subsystem containing several similar or different devices, can an overall self-consistent theory be developed which describes the combined operation of the subsystem?
(5) Using the physics simulations described above, is it possible to define clear operational regimes of acceptable performance to define the functional phase space for the selected devices and subsystems?

Aside from the first question, affirmative answers to these questions signify that the fundamental physics bases of the devices in question are sufficiently well understood that advanced simulations of the devices will be capable of predicting the behavior of the individual devices under specified operational conditions. The subsequent systems engineering assessments and simulations then permit the predicted performance of the overall laser driver system to be evaluated.

3.3.2.2. Heavy Ion driver IFE feasibility

As was described above for the KrF laser driver, there are two parts to the physics feasibility of the Heavy Ion IFE driver:

(1) The physics feasibility of the interaction of the heavy ion beams with the converter plugs to convert the energy efficiently into soft X-rays together with the physics feasibility of the subsequent uniform implosion of the DT target within the Hohlraum, and
(2) the physics feasibility of generating the specified heavy ion indirect-drive target irradiation conditions with regard to heavy ion particle energies, ion beam intensity profiles, directionality, focussed beam diameters, pulse durations, etc.

As mentioned in the previous section, our principal responsibility during the Prometheus Study has been to concentrate on determining the physics feasibility of generating and delivering the 4–6 MJ of heavy ion beam energy in 6 ns pulses in < 6 mm focussed beam diameters at a 5 Hz rate. Included in the second category are the details of fabricating and delivering the indirect-drive heavy ion DT target capsules to a

precise location heavy ion driver irradiation, X-ray conversion, and subsequent DT fuel implosion.

Like the KrF Laser drive described above, the Prometheus Heavy Ion driver design is a complex system composed of a bright Pb^{+2} source, a ramp gradient accelerator, a constant gradient accelerator, storage rings, a bunching accelerator, focusing magnets, self-pinched channel generator, and target injection system which are composed of hundreds of thousands of elements, each of which will be required to perform at specified operating levels for a known length of time. The engineering feasibility described elsewhere in Section 3.3.3 for the heavy ion driver defines the degree to which physically feasible heavy ion driver elements have been designed and engineered in such a manner as to attain performance levels lying within the parameter space defined by the fundamental physics corresponding to the specific element. In order to assess the physics feasibility of the Prometheus Heavy Ion driver design, it is necessary to analyze the fundamental operating principles behind the crucial elements of the heavy ion driver. Typical criteria for establishing the Prometheus Heavy Ion IFE driver physics feasibility are based upon answering the following questions:

(1) Does the intended operational mode of the device violate fundamental physics relationships?
(2) Can a self-consistent theory be developed which is capable of simulating the operation of the device in the ranges of interest?
(3) Do the simulations show that the device can actually operate in the region of phase space of interest?
(4) If a self-consistent theory is developed, are there highly unstable regions in operational phase-space which could produce significant fluctuations or undesired interactions with other systems?
(5) If the device is to be integrated into a subsystem containing several similar or different devices, can an overall self-consistent theory be developed which describes the combined operation of the subsystem?
(6) Using the physics simulations described above, is it possible to define clear operational regimes of acceptable performance to define the functional phase space for the selected devices and subsystems?

The first question asks for a sanity check of the fundamental idea behind the device. The second question eliminates novel ideas which are not sufficiently mature to be developed into a device at the present time. The third question assesses whether or not the range of phase space occupied by the device in operation adequately overlaps the desired performance levels. In general, affirmative answers to questions 2 through 6 signify that the fundamental physics bases of the devices in question are sufficiently well understood that advanced simulations of the devices will be capable of predicting behavior of the individual devices under specified operational conditions. These physics simulations are extremely important in the case of the heavy ion driver since these devices must typically be investigated experimentally at full scale, a fact which can make development of heavy ion drivers very expensive. Providing a fundamental physics models for the heavy ion beam propagation, bunching, neutralization, and self-pinched channel formation are well understood, the subsequent systems engineering assessments and corresponding end-to-end system simulations then permit the predicted performance of the overall heavy ion driver to be evaluated.

3.3.2.3. Summary of KrF laser and heavy ion driver physics feasibilities

Detailed physics analyses and evaluations of the fundamental elements of both the KrF Laser and Heavy Ion drivers have revealed that everything in both designs is consistent with known physics (affirmative answer to question (1) in Sections 3.3.2.1 and 3.3.2.2). There are, however, uncertainties in whether we will be able to operate in the assumed parameter ranges when operating the actual devices. These uncertainties preclude us from guaranteeing that all parts of each driver will work together as a whole to the degree required to meet driver requirements. These uncertainties, in our estimation, can only be resolved by a series of experiments to be performed at a variety of levels. Samples of needed experiments are described in ref. [1] as Research and Development Experiments related to identified Critical Issues. The bottom line is that there appear to be no show stoppers for either the KrF Laser Driver or the Heavy Ion Driver, but some of the required work-arounds could raise the costs of both the laser drivers.

The physics feasibilities of both the KrF Laser and the Heavy Ion drivers are summarized below in Table 12. The rating system assumes the following ranking:

7–9 = demonstrated or easily extrapolated from existing systems,
4–6 = physics feasibility highly probable but needs verification,
1–3 = low physics feasibility except in limited parameter range.

Table 12
Physics feasibilities of laser and heavy ion drivers

No.	Category	Laser	Heavy ion
1	Overall driver	5.8	6.6
1a1	Excimer amplifiers	4	
1a2	Raman accumulators	7	
1a3	SBS pulse compressors	6	
1a4	E/O pulse shaping	5	
1a5	Final focusing	7	
1b1	Injector		7
1b2	Main accelerator		8
1b3	Storage rings		5
1b4	Buncher		7
1b5	Beam transport		6
2	Beam transport	7.3	4.7
2a1	Excimer laser beam quality correction	8	
2a2	Image relaying	8	
2a3	Beam conditioning	7	
2b1	Transport to final focus		7
2b2	Autoneutralized final focus		4
2b3	Channel transport		3
3	Target/beam alignment	3.5	4.5
3a1	Laser beam alignment/overlap	4	
3a2	Target positioning/sensing	3	
3b1	Positioning on target		6
3b2	Channel motion		3
4	Target/driver coupling	3.5	7
4a1	Avoiding Rayleigh-Taylor instabilities	3	
4a2	Efficient inverse Bremsstrahlung absorption	4	
4b1	Efficient conversion in Hohlraum plugs		8
4b2	Generating and focusing soft X-rays		6
5	Target gain	Equal	Equal
Total		5.025	5.7

Based upon our assessments, the heavy ion driver irradiating indirect-drive DT targets has a somewhat higher estimated physics feasibility than does the KrF laser driver irradiating direct-drive DT targets. As can be seen in Table 12, the laser driver physics feasibilities associated with Target/Beam Alignment and Target/Driver Coupling suffers considerably compared with the corresponding feasibilities associated with the Heavy Ion Driver. This major difference in target/beam physics feasibilities is due in part to the considerable technical difficulties in illuminating a moving direct-drive target with a 1% uniformity in the middle of a 5-m radius target chamber.

There is a fundamental connection between the Research and Development Experiments identified in the Prometheus study and estimates of low driver physics feasibilities. By dealing with the high risk physics issues promptly, the goals of inertial confinement fusion research can be met during the first half of the 21st Century.

3.3.3. Engineering feasibility

The engineering feasibility evaluation was performed by several experts within the Prometheus team. Each subcategory was scored by the participants, and an arithmetic average was computed. The subcategory scores were then weighted and summed to obtain total scores. The results are shown in Table 13.

As discussed earlier in Section 3.2, engineering feasibility is broken into two categories: ability to meet design goals and ultimate potential. The heavy ion reactor scored higher in both categories. The total scores were 1.87 and 2.04 for the laser and heavy ion reactor, respectively. Below, some of the reasons for the differences are highlighted.

In general, the heavy ion driver was judged to be easier to build and more reliable. Most of the technology is currently available for the accelerator. One of the largest differences shows up in the engineering simplicity attribute, where the heavy ion reactor scores much higher. For the same reasons, cost projections were felt to be more credible for the heavy ion reactor.

Several components of the laser reactor provide uncertainty in fabrication and performance. The final optics appears much more problematic. The large size, vulnerability to the blast effects, and difficulty with shielding lead to lower scores.

The use of the same cavity design concept for the two reactors tended to reduce the differences. However, the large number of beamline penetrations for the laser reactor make it considerably less attractive. The smaller size of the heavy ion reactor makes fabrication easier, but uncertainties due to the higher power density offsets this advantage.

The use of direct vs. indirect drive targets did not lead to large differences in engineering feasibility. The impact of target choice is probably felt more strongly in the physics feasibility.

For both reactor designs, the Engineering Feasibility scoring for safety was very high. The scores for long-term activation were also relatively high, but somewhat lower than for safety. This is due to the presence of Pb and to uncertainties in predicting impurity levels and in the nuclear data.

3.3.4. Economic comparison and evaluation

This comparison and evaluation parameter will judge the relative economic basis between the two

Table 13
Engineering feasibility evaluation

	Weight	Weighted L score	Weighted HI score
Ability to meet design goals			
1. Component fabricability			
first wall	0.021	0.029	0.029
blanket	0.012	0.020	0.020
driver	0.009	0.017	0.023
beam transport	0.009	0.018	0.025
final optics	0.009	0.021	0.023
2. Subsystem performance goals			
2.1 Cavity			
2.1.1 First wall protection	0.036	0.050	0.054
2.1.2 Blanket	0.036	0.086	0.086
2.2 Fusion reaction support systems			
2.2.1 Driver	0.0216	0.038	0.050
2.2.2 Beam transport	0.0216	0.043	0.047
2.2.3 Final optics	0.0216	0.032	0.047
2.2.4 Target fabrication	0.0216	0.043	0.040
2.2.5 Target injection	0.0216	0.043	0.036
3. Tritium fuel self-sufficiency	0.12	0.18	0.18
4. Reliability goals			
first wall	0.021	0.032	0.032
blanket	0.012	0.021	0.021
driver	0.009	0.017	0.023
beam transport	0.009	0.014	0.023
final optics	0.009	0.012	0.021
5. Maintainability			
first wall	0.021	0.042	0.045
blanket	0.012	0.028	0.030
driver	0.009	0.024	0.020
beam transport	0.009	0.018	0.018
final optics	0.009	0.015	0.015
6. Lifetime goals			
first wall	0.021	0.032	0.032
blanket	0.012	0.021	0.021
driver	0.009	0.014	0.023
beam transport	0.009	0.014	0.016
final optics	0.009	0.014	0.014
7. Cost projections			
cavity	0.015	0.019	0.019
driver	0.015	0.026	0.035
target manufacture	0.015	0.026	0.035
BOP	0.015	0.036	0.036
Ultimate potential			
8. Potential for inherent safety	0.1	0.270	0.275
9. Potential for low long-term activation	0.1	0.200	0.192
10. Engineering simplicity			
individual system complexity	0.06	0.105	0.160
interdependence of systems/functions	0.06	0.090	0.120

Table 13 (continued).

	Weight	Weighted L score	Weighted HI score
11. Operating requirements	0.04	0.080	0.080
12. Potential for enhanced energy conversion eff.	0.04	0.080	0.080
TOTALS			
Design goals		1.047	1.131
Ultimate potential		0.825	0.907
TOTAL		1.872	2.038

reactor conceptual designs. Eventually this economic parameter will be the only meaningful measure to be used by utilities to judge the relative merit of opposing designs. As the experimental devices and the demonstration plants are developed and operated, the physics and engineering feasibility questions will have all been resolved in a positive or a negative manner. The R&D criteria is a measure to scope the money and effort required to realize the goal of commercial fusion. All other criteria and judgement factors such as safety will eventually be measured and compared in economic terms. A present example is that of an allowance for the decommissioning of the reactor. The plant with the lower environmental risk has a lesser cost factor for the decommissioning effort.

The criterion to be employed in this present Economic Comparison will be the cost of electricity (COE). This is a meaningful figure of merit in that it combines many aspects of the plant into a single value. The component factors are weighted according to the cost structure employed in the US utilities. The structure of the COE determination is as follows:

$$\mathrm{COE} = \frac{[\text{Annualized Capital Cost} + \text{Yearly Operating Cost}]}{\text{Net Power} \times \text{Plant Availability}},$$

$$\mathrm{COE} = \frac{[\text{Annualized Capital Cost} + \text{Yearly Operating Cost}]}{[\text{Thermal Pwr} \times \text{Efficiency} - \text{Aux Pwr}] \times [1 - \text{SchedDowntime} - \text{MTBF} \times \text{MTTR}]}$$

This equation combines the effects of the capital costs of the entire plant facility as well as the time it takes to construct the plant. The capital costs emphasize choice of materials, design optimization, and cost efficient processes. The yearly operating costs include the operating and maintenance staffs, fuel costs, and the maintenance and supply costs. These costs are offset by the production of energy sold to the distribution grid. To generate net power, thermal energy must be produced thus emphasizing utilization of high quality energy conversion, high gain targets, high neutron and energy multiplication in the blankets, and efficient use of materials. Plant availability stresses minimizing the downtime, both the scheduled and the unscheduled. Reliability and maintainability of future systems is very difficult to predict.

Before the specific COE values are revealed, several comments should be discussed. Although one reactor design concept may show more favorable values of COE over the other concept, there are many competing and generally offsetting factors which should be recognized and considered.

Capital costs are strong drivers – The most influential cost elements are the drivers, the beamlines, the power supplies, and the reactor cavities. The heavy ion driver has the deserved reputation of being a very costly driver. Our team took an innovative approach to minimize the cost of the heavy ion driver and succeeded in reducing the cost of the HI driver to less than that of the laser driver. The many laser beamlines required for symmetric illumination also contributed toward the higher cost of the laser plant. The quality of the laser driver power supplies implied a higher cost for the laser system. The lower system efficiency of the laser system caused a larger demand for recirculating power, and hence, more thermal power, more reactor plant equipment, more turbine plant equipment, more electric plant equipment and so on. Plant elements with a minor cost influence included the fuel cycle, the target factory, general-purpose buildings and the shielding. Elements with slight influences were the reactor cavity and remote handling which did not significantly affect either candidate concept.

Operating costs did not have a significant impact – The level of definition in these studies did not offer any discernible differences in the operating costs between these two conceptual designs. The operating costs for the direct drive targets are nearly equal to the indirect target costs. The targets are cheaper but more are required due to the higher repetition rate. An

Table 14
Safety and environment comparison

Category	WT	L	HI	Rationale
Source term characterization	30%			
Source term in target factory	0.2	1.	1.	No difference at the level of this study
Source term in the first protection chamber wall	0.2	1.	1	No difference at the level of this study
Source term in the breeding blanket and shield	0.2	1.	1.	No difference at the level of this study
Source term in the driver	0.2	1.	0.83	The heavy ion beam will activate the material in the beam tunnel
Non-radiological sources (fluorine)	0.2	0.75	1.	The fluorine for the laser has no counterpart in the heavy ion
Total source term characterization:		0.95	0.97	
Response to accidents (fault tolerance)		30%		
Response to LOCA and LOFA in the first protection chamber wall	0.12	1.	1.	No difference at the level of this study
Response to LOCA and LOFA in the breeding blanket and shield	0.12	1.	1.	No difference at the level of this study
Response to beam/pellet misfire accident in the chamber wall	0.12	1.	0.9	The loss of one of the two heavy ion beams will have greater effect than the loss of one of the laser's 60 beams
Response to loss of coolant in the final optics or focusing magnet or vacuum pumping systems	0.12	1.	1.	No difference at the level of this study
LOCA in driver system	0.12	1.	0.83	The loss of one of the two heavy ion beams will have greater effect than the loss of one of the laser's 60 beams
Fault tolerance to loss of T_2 and D_2 containers	0.1	1.	1.	No difference at the level of this study
Fault tolerance to containment integrity	0.1	1.	1.	No difference at the level of this study
Fault tolerance to target factory integrity	0.1	1.	1.	No difference at the level of this study
Fault tolerance to driver system	0.1	1.	1.	No difference at the level of this study
Total response to accidents:		1.	0.97	
Non-accident concerns	40%			
Occupational exposure (regular, maintenance)	0.25	1.	0.75	The heavy ion beam will activate the material in the beam tunnel
Routine radioactive emission rate	0.25	1.	1.	No difference at the level of this study
Waste disposal (radiological, hazardous, mixed)	0.20	1.	0.75	The heavy ion will activate the material in the beam tunnel, causing more waste disposal
Non-radiological hazards (fluorine, lead)	0.15	0.5	1.	The fluorine for the laser has no counterpart in the heavy ion
Heat dissipation	0.10	0.9	1.	A greater amount of power is needed to drive the laser, with a corresponding greater amount of waste heat to be dissipated
Construction impacts (environmental)	0.05	1.	0.75	The long heavy ion beam tunnel has no laser counterpart
Total non-accident conditions:	0.92	0.88		
Total safety and environment comparison:	0.95	0.93		

indirect target may be an option for the laser driven-plant but future target designs may significantly impact the performance of the targets which would outweigh the perceived cost differences.

Net thermal power is a split decision – The higher gain of the direct drive target tends to favor the laser driver for the same energy level. However the more efficient LINAC driver better utilizes the available target yields requiring less recirculating power be generated, thus delivering more net energy to the electric grid.

Overall efficiency is credited to the Heavy Ion driver – The higher system efficiency of the heavy ion LINAC makes better use of the driver energy, holds the size of the other plant equipment to a minimum, and maximizes the plant output for a given level of fusion and thermal plant output. Both reactor concepts have been designed with high temperature primary coolant in order to maximize the thermal efficiency conversion. Since the laser driver is recognized as the less efficient system, the waste heat associated with the KrF gas flow loops is used as an additional source of energy which is directed into the thermal conversion system to increase the overall system efficiency.

Low auxiliary power helps the efficient use of energy – The LINAC has the advantage of requiring less auxiliary power delivered back into the LINAC. All other plant factors are generally even for this factor.

Scheduled downtimes are nearly equal – It is believed that the Heat Transfer and Transport System, the Turbine Plant Equipment, and the Reactor Cavity are the systems which will require the majority of the scheduled downtime for the plant. The steam generator and the turbines will require routine preventative maintenance. The reactor cavity will have components with limited lifetimes which need periodic replacement. The laser mirrors and optics are designed for long lifetimes and only the final optics may need replacement a few times during the plant lifetime. The heavy ion driver components are designed for the life of a plant.

The unscheduled downtime is determined by the MTBF and MTTR – The Mean Time Between Failures (MTBF) is again driven by the systems mentioned above which have large scheduled downtimes, namely the Heat Transfer and Transport, Turbine Plant Equipment, and the Reactor Cavity. In addition, the Driver Plant Equipment will contribute to the unscheduled downtime. The laser amplifiers may have some failures, but these can be accommodated without causing a shutdown of the reactor. If a mirror or lens must be replaced, it can be quickly replaced with a low mean time to repair (MTTR). The LINAC components are more reliable but any failures of the main beamline elements would cause a shutdown of the entire reactor until the element is repaired. The net result of scheduled and unscheduled downtime is assessed in inherent availability which slightly favors the heavy ion design.

In summary, the factors which contribute toward final economic evaluation are comprised of many terms which are not black and white issues. Both reactor and driver concepts have perceived advantages and disadvantages as viewed with today's spectacles. But technology marches ahead, making twists and turns, driven by market pressures, political maneuvers, and societal influences. We believe these studies have suggested some innovative and cost-effective solutions to existing problems and we believe there are even better solutions yet to be uncovered!

Results of the economic evaluation – The cost of electricity for the two reactor concepts indicate that the heavy ion driven-reactor would be somewhat more attractive than the KrF laser driven-reactor, as shown below:

Reactor concept	Cost of electricity
Heavy Ion driven	62.6 mill/kWh
KrF Laser driven	72.0 mill/kWh

3.3.5. Safety and environment

In performing the Safety and Environment comparison, the evaluation criteria were first divided into three general categories, with a weighting factor assigned to each category, as follows: (1) Source Term Characterization (30%), (2) Response to Accident (Fault Tolerance) (30%), and (3) Non-Accident Concerns (40%). With these factors, accident conditions receive substantially more weight in the comparison (60%), than do normal operation factors (40%). Next, each of the three general categories was further divided into subcategories, as indicated on Table 14. As with the general categories, the subcategories were assigned weighting factors.

Each reactor design (laser or heavy ion) was then assigned a relative score for each subcategory. The design that has the least adverse impact for a subcategory is given a score of 1.0, while the score for the other design is based on how severe its impacts are relative to the least adverse design. For example, if the laser design is judged to have impacts which are twice as severe as the heavy ion design, then the heavy ion is assigned a score of 1.0, while the laser design is given a

0.5 score. If both designs are judged to be equal in their impacts of a subcategory, then both are given a score of 1.0.

Using this methodology, Table 14 presents the results of the safety and environment comparison. A brief rationale for the assignment of the scores is provided for each category. As shown, the laser design is slightly preferred over the heavy ion design. However, at the level of this study, the difference is not considered to be significant, and the two designs should be considered to be equal with regards to safety and environment.

3.3.6. R&D requirements

An R&D assessment has been carried out for Prometheus-L and H. Because of limitations on time and resources available for this study the assessment has not attempted to develop comprehensive R&D plans. Rather, the effort was limited to identifying the R&D required to resolve the key technical issues identified for Prometheus. A specific development goal was selected as the ultimate objective of the R&D identified in this effort. This goal is to develop the physics and engineering data base sufficient to construct an IFE Experimental Power Reactor (IEPR). An IEPR is envisioned as a facility in which the basic physics and engineering performance as well as system integration tests are carried out. It will have prototypical components and will probably produce several hundred megawatts of fusion power and operate with about one pulse per second and overall availability of about 20–30%.

The R&D assessment focused primarily on critical components unique to IFE: target, driver, and cavity. Some modest R&D has also been identified for the tritium system and safety.

The evaluation methodology for the R&D category requires evaluation of costs (capital and operating), time, and risk. Since a comprehensive R&D assessment was not within the scope of this study, complete data was not available to rigorously follow the evaluation methodology.

The key items of the R&D costs are shown in Table 15. The costs for laser and heavy ion drivers are comparable with the heavy ion reactor concepts having a modest advantage in lower cost. The time it takes to perform the required R&D does not appear to be a significant discriminating factor for the R&D items evaluated in this study.

3.3.7. Overall evaluation

A summary of the scores for the figures-of-merit of the five evaluation areas is given in Table 16 for the laser-driven and heavy-ion driven reactors. The scores were normalized so that higher numbers mean better scores. Two key conclusions can be made based on the overall evaluation analysis and the scores in Table 16:

(1) The heavy-ion driven reactors appear to have an overall advantage over laser-driven reactors.
(2) However; the differences in scores are not large and future results of R&D could change the overall ranking of the two IFE concepts.

Table 15
Summary of key items of costs (capital plus operating) of R&D for laser and heavy ion reactors

	Laser (M$)	Heavy ion (M$)
Cavity		
First wall protection	175	175
Blanket	273	273
Shield	60	50
Target and driver		
Driver	825	805
Target (for both)	235	235
Target (driver-target)	300	200
Tritium	30	30
Safety and environment (specific items)	20	20
Total (for items shown)	1918	1788

4. Summary

A comprehensive list of critical issues identified for the Prometheus IFE conceptual designs has been analyzed and characterized. Each critical issue contains several key physics and engineering issues associated with the major reactor components and impacts key

Table 16
Summary of scores for the five evaluation areas

Evaluation area	Score *	
	Laser-driven	Heavy ion-driven
Physics feasibility (P)	50	57
Engineering feasibility (G)	85	93
Economics (C)	68	78
Safety and environment (S)	95	93
RandD requirements (D)	52	56

* Score normalized so that higher numbers mean better scores.

aspects of feasibility, safety, and economic potential of IFE reactors. Some critical issues have some commonality with MFE, e.g., radiation shielding; fabricability, reliability and lifetime of SiC structure; and tritium self-sufficiency. Another critical issue deals with the ability to demonstrate moderate gain at a low driver energy, which may be crucial to the IFE pathway to commercial fusion. Various aspects of target and driver development are critical to the success of IFE.

A quantitative methodology for the comparison and evaluation of the two reactor designs has been developed. The general evaluation parameters include: (1) Physics Feasibility; (2) Engineering Feasibility; (3) Economics; (4) Safety and Environment; and (5) Research and Development Requirements. Specific figures of merit were established for each category and applied to each reactor design.

In the Physics Feasibility area, the heavy ion driver option is judged to be slightly more feasibile with pulses in Overall Driver, Target/Beam Transport, and Target/Driver Coupling. The laser option is favored in the areas of Beam Transport.

The Engineering Feasibility was evaluated in two areas, the ability to meet the design goals and the ultimate potential. The heavy ion design option scored higher in both categories. The heavy ion option's ability to meet the design goals was judged to be 8% better, and the ultimate potential scored 10% better.

The Economic Comparison shows the heavy ion driver option to have roughly a 13% lower cost of electricity. The cost of electricity has many factors including capital cost, operating cost, net power, and plant availability. None of the individual factor differences exceeds a percent or two, but they all favor the heavy ion concept in the economics category.

The Safety and Environment Comparison was essentially a draw with the laser having slightly higher scores. The heavy ion option scored slightly higher in the Source Term Characterization, whereas the laser option scored better in the Response to Accidents and Non-Accident Conditions.

The Research and Development assessment considered the cost and time to conduct the R&D for the critical components. The figure of merit for this assessment was the summation of the capital and operating costs for the related R&D programs. The total costs for both options were reasonably close with only 7% separating the two options. The heavy ion reactor option was judged to have a modest advantage due to the low R&D costs.

Overall, the heavy-ion driven reactors appear to have an advantage over laser-driven reactors. However, the differences in scores are not large and future results of R&D could change the overall ranking of the two IFE concepts.

Acknowledgements

The work presented here is based on the Prometheus studies, which is led by McDonnell Douglas Aerospace. Other participants include Canadian Fusion Fuels Technology Project, Ebasco Services, Inc, KMS Fusion, Inc, SPAR Aerospace, Ltd, TRW Space and Electronics Division, and the University of California, Los Angeles. In addition, an Oversight Committee and a Target Working Group have provided assistance throughout the study.

This study was supported by the US Department of Energy/Office of Fusion Energy, under the prime contract DE-AC02-90ER54101 to McDonnell Douglas Aerospace and under subcontract to UCLA, TRW, and KMS Fusion, Inc.

References

[1] L. Waganer et al., Inertial Fusion Energy Reactor design studies: Prometheus-L and Prometheus-H, McDonnell Douglas Company Report, MDC 92E0008/DOE/ER-54101 (March 1992).

[2] National Energy Strategy, First Edition 1991/1992, U.S. Department of Energy, Washington, DC (February 1991).

[3] W.J. Hogan, Small Inertial Fusion Energy (IFE) Demonstration Reactors, in: Proceedings 14th IEEE/NPSS Symposium on Fusion Engineering, San Diego, CA, October 1991 (to be published).

[4] W.J. Hogan, Private communication (1992).

[5] W.L. Kruer, The Physics of Laser Plasma Interactions, Chapter 5: Collisional absorption of electromagnetic waves in plasma, pp. 45–56.

[6] J.J. Thomson, C.E. Max, J. Erkkila and J.E. Tull, Laser light absorption in spherical plasmas, Physical Review Letters 37 (1976) 1052–1056.

[7] Nova Upgrade facility for ignition and gain, LLNL IFE Program, UCRL-LR-106874, LLNL, Livermore, CA 94551 (March 1991).

[8] Nova Upgrade – a proposed IFE facility to demonstrate ignition and gain by the year 2000, LLNL IFE Program, UCRL-LR-106736, LLNL, Livermore, CA 94551 (March 1991).

[9] R.C. Davidson et al., Inertial Confinement Fusion Reactor design studies; Recommended guidelines, prepared for the Department of Energy Office of Fusion Energy (September 1990).

[10] Revised target information for IDF reactor studies, received from Roger Bangerter, Lawrence Berkeley Laboratory, Bldg. 47, room 112 (28 February 1991).
[11] New techniques for KrF laser fusion systems, Interim Report for Los Alamos National Laboratory, pp. 2-70 through 2-72, Los Alamos, New Mexico, written by Dr. M. Kuschner, then at Spectra Technology, Inc., Seattle, Washington.
[12] M.A. Abdou et al., Deuterium–tritium fuel self-sufficiency in fusion reactors, Fusion Technol. 9 (March 1986) 250–284.
[13] G.J. Linford, E.R. Peressin, W.R. Sooy and M.L. Spaeth, Very long lasers, Applied Optics 13 (1974) 379–390.
[14] L.A. Rososha et al., Aurora multi-kJ KrF laser system prototype for IFE, Fusion Technol. 11 (1987) 497–531.
[15] M. Kuschner et al., New techniques for KrF laser fusion systems, Interim Report for Los Alamos National Laboratory, Spectra Technologies, Inc., Seattle, WA (1986).
[16] M.A. Abdou, P.J. Gierszewski, M.S. Tillack et al., Technical issues and requirements of experiments and facilities for fusion nuclear technology, Nuclear Fusion 27, no. 4 (1987) 619–688.
[17] M.A. Abdou et al., A study of the issues and experiments for fusion nuclear technology, Fusion Technol. 8, no. 3 (November 1985) 2595–2645.
[18] Blanket Comparison and Selection Report, Interim Report, ANL, FPP-83-1(1983), and Final Report, ANL/FPP-84-1 (1984).